European Transport Studies 2 (2025) 100029

Contents lists available at ScienceDirect

European Transport Studies

journal homepage: www.sciencedirect.com/journal/european-transport-studies

Will e-bikes revolutionize urban mobility? Development and application of a transport model differentiating between conventional and electric bicycle traffic☆

Leonard Arning *, Heather Kaths

Chair of Bicycle Traffic, University of Wuppertal, Pauluskirchstraße 7, Wuppertal, 42285, NRW, Germany

ARTICLE INFO

Keywords:
Bicycle traffic
Cycling
e-bike
Infrastructure
Transport model
Macroscopic
Mode shift

ABSTRACT

Increasing cycling is crucial for building sustainable cities. Electric bicycles reduce the physical effort required for cycling, particularly in hilly areas and for individuals with limited strength, contributing to lower car use and promoting social equity. However, current transport models often overlook the growing impact of electric bicycles on urban mobility. We present a macroscopic transport model for Wuppertal, Germany, the first to dynamically differentiate between conventional and electric bicycles across ownership, mode, and route choice. Our model incorporates bicycle infrastructure, gradient, motor vehicle speed, and turns in value of distance space. In ownership and mode choice, differences in preference between person groups and trip purposes are considered.

While the differentiated modeling approach did not improve the quality of the model compared to a model not differentiating between conventional and electric bicycle traffic, it provides valuable analytical insights. We evaluated three scenarios related to building more bicycle infrastructure and increasing e-bike ownership. Our results confirm that adding infrastructure increases cycling, although to a small degree. Infrastructure expansion primarily increases conventional bicycle use, whereas promoting electric bicycle ownership leads to a strong increase in electric bicycle trips, mostly replacing car trips. Synergies between electric bicycle adoption and infrastructure expansion are minimal but may vary depending on the characteristics of the latter. Furthermore, infrastructure expansion provides substantial benefits for existing cyclists beyond mere travel time savings. Our findings highlight the importance of integrating e-bikes into transportation models to accurately assess their impact on urban mobility and guide effective policy development.

1. Introduction

Increasing cycling is an effective strategy to make cities more sustainable and socially resilient. In recent years, electric bicycles (e-bikes) have gained popularity alongside conventional bicycles (c-bikes), especially in Europe and North America. Due to the electric assistance provided by e-bikes, cycling requires less physical exertion, which is particularly relevant in hilly cities, for longer trips, and for individuals with lower physical strength, such as older adults. E-bikes thus not only substitute for c-bike travel but also contribute to an overall increase in cycling, often displacing other modes of transportation. Therefore, e-bikes fundamentally change the role of cycling as a utilitarian mode of transport by reducing transport-related greenhouse gas emissions, contributing to more livable cities, and supporting social equity.

To analyze, forecast, and optimize transportation infrastructure, policies, and operations, cities use transport models. A transport model is a computational representation of a transportation system that simulates travel demand and the flow of traffic through a network. It consists of several sub-models, most commonly traffic generation, destination choice, mode choice, and route choice. Transport models used in practice largely neglect the electrification of bicycle traffic (Arning et al., 2023). This gives rise to several issues: models might be less accurate overall, they might underestimate future rates of cycling and the impact of measures such as new cycling infrastructure, and they cannot be used to analyze e-bike-specific policies. This study addresses the following research questions: How can existing strategic transport models be enhanced to better reflect differences between c-bikes and e-bikes? Does model quality improve compared to an undifferentiated

☆ We would like to thank the City of Wuppertal for providing the base model for our work as well as survey and traffic count data. This research was supported via funding from the German Federal Ministry of Digital and Transport's Bicycle Traffic Endowed Professorship at the University of Wuppertal.

* Corresponding author.
E-mail addresses: arning@uni-wuppertal.de (L. Arning), kaths@uni-wuppertal.de (H. Kaths).

https://doi.org/10.1016/j.ets.2025.100029
Received 1 April 2025; Received in revised form 21 July 2025; Accepted 30 July 2025
Available online 9 August 2025

bicycle mode? And are there e-bike specific effects of interventions aimed to promote cycling? To answer these questions, we develop a transport model for a hilly city that fully differentiates between c-bikes and e-bikes, identify practical problems in implementing such a modeling approach, assess the impact on model quality, and investigate the effects of e-bike availability and cycling infrastructure as well as interaction effects.

1.1. Literature on transport model application

In this section, we provide an overview of academic publications on transport models with a focus on cycling. For a review of non-academic modeling practice, we refer to Arning et al. (2023). There, only two models were identified that consider the electrification of bicycle traffic, both falling short of modeling c-bikes and e-bikes as two distinct modes of transport throughout all sub-models.

We identified 15 relevant works on the development of transport models with a focus on cycling. We restrict our review to publications since 2017 because before that, bicycle-style e-bikes were still in the phase of early-adoption. They are summarized in Table 1. For comparison, we also include a brief description of the work we present in this paper at the bottom of the table. In three cases, multiple publications use the same model. Three out of twelve models are agent-based. The others use flow-based approaches, most commonly using the software PTV Visum. Only three model areas are outside of Europe. We note that in South and East Asia, the term e-bike is often used to refer to electric motorbikes, which are not considered here.

Bicycle **ownership** is considered in only one publication (Hebenstreit, 2021), where it is an attribute assigned to agents with fixed probabilities based on survey data. For **mode choice**, several approaches can be identified. In five models, no dynamic mode choice takes place. Instead, bicycle trip matrices are generated from observed data (Jacyna et al., 2017; de Melo and Isler, 2023; Kaziyeva et al., 2021), obtained from a separate model (Argyros et al., 2024), or mode shares are exogenous scenario variables (Fan and Harper, 2022). In the other seven models, some kind of impedance for bicycle traffic for origin–destination (OD) pairs is defined, which is then used to dynamically model mode shares. Three models use Nested Logit, with mode choice taking place at the nesting level before (Liu et al., 2020) or after (Hallberg et al., 2021; Paulsen and Rich, 2023) destination choice. Two models (Oskarbski et al., 2021; van Dulmen and Fellendorf, 2021) use Multinomial Logit (MNL), neither differentiating by person groups nor trip purposes. In the two MATSim models (Hebenstreit, 2021; Jafari et al., 2022), MATSim's standard scoring and routing parameters (Ziemke et al., 2019) are used.

With two exceptions (Argyros et al., 2024; Fan and Harper, 2022), all models implement some kind of **route choice**. In seven cases, the demand for each origin–destination pair is assigned to the route with the lowest impedance (Jacyna et al., 2017; Liu et al., 2020; Hallberg et al., 2021; Paulsen and Rich, 2023; de Melo and Isler, 2023; Kaziyeva et al., 2021; Jafari et al., 2022). In the other cases, a stochastic assignment or agent routing distributes demand across several suitable routes (Oskarbski et al., 2021; van Dulmen and Fellendorf, 2021; Hebenstreit, 2021).

All but three publications (Jacyna et al., 2017; Kaziyeva et al., 2021; Jafari et al., 2022) **evaluate an intervention**. In some cases, models are used to evaluate the impact of an exogenous mode shift (Fan and Harper, 2022; van Dulmen and Fellendorf, 2021; Hebenstreit, 2021), improving surface quality (Argyros et al., 2024), or expanding a c-bike and e-bike sharing system (Hebenstreit, 2021). Most often, an expansion of bicycle infrastructure is evaluated (Liu et al., 2021; Oskarbski et al., 2021; Rich et al., 2021; Paulsen and Rich, 2023, 2024; de Melo and Isler, 2023; van Dulmen and Fellendorf, 2021; Hebenstreit, 2021). For Copenhagen, two works evaluate ambitious expansions of an existing cycling superhighway network (Rich et al., 2021; Paulsen and Rich, 2024). They do not report modal shifts, but substantial health benefits due to an increase in distance cycled, leading to benefit-cost ratios of up to 21.37 (Paulsen and Rich, 2024) and a rate of return on investment of up to 0.23 (Rich et al., 2021). Three other sources report more detailed data on mode shift, indicating more modest results: In Vienna, the modal split for cycling increases by only 0.1%p due to three new fast cycle routes (Hebenstreit, 2021). In Gdynia, six infrastructure measures ranging from a seaside bicycle path in a suburb to a new bicycle bridge across the harbor result in increases in the number of bicycle trips (not modal split) of 0.24% and 1.24%, respectively (Oskarbski et al., 2021). Lastly, model results show that several infrastructure investments in central Stockholm mainly attract bicycle trips from other routes, with the increase in bicycle trips due to mode shift in each location being only between 0.8% and 5.5% (Liu et al., 2021).

1.2. Literature on bicycle impedance

Impedance represents the resistance of distance, time, comfort, and other influencing factors across a route or OD pair to traveler's decisions. It is the core and sometimes sole component of utility formulations for destination, mode and route choice. This subsection reviews the typical factors included.

In the transport models discussed in the previous section, impedance includes either distance or time, corresponding to value-of-distance (VoD) or value-of-time (VoT) space, respectively. When VoD incorporates factors beyond distance, link attributes, such as infrastructure, can alter the perceived length of a link (Liu et al., 2020; van Dulmen and Fellendorf, 2021). Clearly, a link's objective length is not altered due to the type of facility (e.g., bicycle path or in mixed traffic), but the willingness of cyclists to make detours for more preferable infrastructure can be expressed by parameters in VoD space. When including additional factors in VoT, no publication did so to account for subjective differences only. Instead, three studies refine impedance functions to more accurately model objective speed and travel time, for example, by including gradient in speed functions (Liu et al., 2020; Oskarbski et al., 2021; Hallberg et al., 2021; Paulsen and Rich, 2023; de Melo and Isler, 2023), and three other studies present at least one impedance function that combines subjective and objective influences in VoT (Liu et al., 2020; de Melo and Isler, 2023; Hebenstreit, 2021). Factors included in impedance beyond distance and time are bicycle infrastructure (Liu et al., 2020; Oskarbski et al., 2021; Hallberg et al., 2021; Paulsen and Rich, 2023; de Melo and Isler, 2023; van Dulmen and Fellendorf, 2021; Hebenstreit, 2021; Kaziyeva et al., 2021), gradient (Oskarbski et al., 2021; de Melo and Isler, 2023; van Dulmen and Fellendorf, 2021; Hebenstreit, 2021), road surface (Oskarbski et al., 2021; Argyros et al., 2024; Kaziyeva et al., 2021), intersections (Hallberg et al., 2021; Paulsen and Rich, 2023; de Melo and Isler, 2023), and car traffic volume (van Dulmen and Fellendorf, 2021; Kaziyeva et al., 2021). Three studies differentiate impedance based on personal characteristics (Hallberg et al., 2021; Paulsen and Rich, 2023; Hebenstreit, 2021).

In most cases, mode choice impedance mirrors route choice impedance. There are three exceptions where bicycle mode choice includes additional parameters that are not part of route choice impedance (Hallberg et al., 2021; Hebenstreit, 2021; van Dulmen and Fellendorf, 2021). In another exception, one tested route choice impedance includes more factors than mode choice (van Dulmen and Fellendorf, 2021). Generally, it is advisable to include all factors from route choice impedance in mode choice, as indicator matrices (including mode choice impedance) for are calculated based on optimal routes between origins and destinations. For instance, if route choice impedance would account for infrastructure but mode choice would not, new infrastructure may attract trips from parallel routes, increasing trip length and consequentially reducing mode share on that route.

Lastly, we summarize additional academic literature that investigates bicycle route choice using stated or reveled preference data in

Table 1
Literature on the application of bicycle transport models.

Source	Model type, software	Area	Differentiation c-bike/e-bike	Bicycle ownership	Bicycle mode choice	Bicycle route choice	Intervention
Jacyna et al. (2017)	Macroscopic, Visum	Warsaw	None	None	None, fixed generation rates from survey data.	Shortest distance via bicycle permissible links.	none
Liu et al. (2020, 2021)	Macroscopic, TransCAD	Stockholm	None	None	NL across trip generation, mode, and destination choice. Same impedance as route choice.	Three impedance formulations tested: travel distance, infrastructure, and travel time (observered and modeled speed). Fastest route.	Infrastructure expansion
Oskarbski et al. (2021)	Macroscopic, Visum	Gdynia	None	None	MNL. Same impedance as route choice.	Travel time calculated using empirical link speed function, based on infrastructure, gradient and surface. Stochastic assignment.	Infrastructure expansion
Hallberg et al. (2021), Rich et al. (2021)	Macroscopic, Traffic Analyst for ArcGIS	Copenhagen	E-bike share among cycling is scenario input, affecting average speed of cycling.	None	NL across destination and mode choice. Same impedance as route choice with added dummies.	Travel time calculated from empirical link speeds differentiated by bicycle type, infrastructure, three preference groups, and intersection delay. Fastest route.	Infrastructure expansion
Paulsen and Rich (2023, 2024)	Macroscopic, Traffic Analyst for ArcGIS	Copenhagen	None	Simplified version of Hallberg et al. (2021)'s model.			Infrastructure expansion
Argyros et al. (2024)	Macroscopic, Traffic Analyst for ArcGIS	Copenhagen	None	Bicycle traffic demand not modeled in this work, static link flow is based on COMPASS model.			Improve surface quality
Fan and Harper (2022)	Macroscopic, Visum	Seattle	None	None	Cycling penetration is manual scenario variable.	None	Exogenous modal shift
de Melo and Isler (2023)	Macroscopic, Visum	Sao Paulo	None	None	None, bicycle trip matrix modeled based on traffic counts.	Three impedance formulations tested: travel distance, travel time (including infrastructure and gradient), or suitability (like travel time, plus subjective impacts of gradient, infrastructure, stop signs, and turns), respectively. Fastest/shortest route.	Infrastructure expansion
van Dulmen and Fellendorf (2021)	Macroscopic, Visum	Graz	None	None	MNL. Impedance includes distance and elevation.	Two impedance formulations tested: distance, gradient, infrastructure, and car traffic volume (original), and distance only (simplified). Stochastic assignment.	Infrastructure expansion, exogenous modal shift
Kaziyeva et al. (2021)	Agent-based, GAMA RC1.8 platform	Salzburg	None	None	None, static mode shares.	Two impedance formulations tested: distance and safety. Safety index (infrastructure, car traffic volume, surface) based on Loidl and Zagel (2014), unclear whether VoD or VoT. Fastest/safest route.	None

(*continued on next page*)

Table 1 (*continued*).

Source	Model type, software	Area	Differentiation c-bike/e-bike	Bicycle ownership	Bicycle mode choice	Bicycle route choice	Intervention
Hebenstreit (2021) (Case study in Chapter 7 only)	Agent-based, MATSim	Vienna	Desired speed and impact of gradient differs by bicycle type. For shared e-bikes, battery status is modeled.	C-bike/e-bike ownership assigned to agents based on survey data	Impedance includes gradient, safety, comfort, capacity, and speed (not link-specific but derived from link type). Scoring and routing parameters based on Ziemke et al. (2019).		Infrastructure expansion, bike-sharing system, exogenous modal shift
Jafari et al. (2022)	Agent-based, MATSim	Melbourne	None	Unclear	Impedance unclear. Scoring parameters based on Ziemke et al. (2019). Routing via shortest path.		none
This work	Macroscopic, Visum	Wuppertal	Full separation between c-bikes and e-bikes throughout ownership, mode, and route choice.	C-bike/e-bike ownership from discrete choice model.	MNL. Same impedance as route choice with added dummies for person group and trip purpose.	Impedance accounting for distance, infrastructure, gradient, car speed, and turns. Stochastic assignment.	Infrastructure expansion, exogenous increase in e-bike ownership.

Table 2. For a recent and thorough review, we refer to Łukawska (2024). For additional factors relevant to mode choice, namely person groups and trip purposes, we refer to Section 3.4.

MNL and Path Size Logit (PSL) are the most commonly used, with the latter addressing the former's independence from irrelevant alternatives problem by taking into account similarity between routes (overlaps). Almost all sources take into account bicycle infrastructure and distance, with the exception of Dane et al. (2020) and Hardinghaus and Weschke (2022, 2023), respectively. Eleven sources consider aversion to turns, intersections, or specific types of these elements (Broach et al., 2012; Prato et al., 2018; Koch and Dugundji, 2021; Scott et al., 2021; Shah and Cherry, 2021; Cho and Shin, 2022; Łukawska et al., 2023; Meister et al., 2023; Rupi et al., 2023; Khavarian et al., 2024; Meister et al., 2024). Aspects of topography are considered in nine works (Broach et al., 2012; Huber et al., 2021; Scott et al., 2021; Cho and Shin, 2022; de Jong et al., 2023; Łukawska et al., 2023; Meister et al., 2023; Khavarian et al., 2024; Meister et al., 2024). Motor vehicle speed limits are included in eight models (Broach et al., 2012; Huber et al., 2021; Shah and Cherry, 2021; de Jong et al., 2023; Hardinghaus and Weschke, 2022, 2023; Meister et al., 2023, 2024) and pavement surface in six models (Prato et al., 2018; Huber et al., 2021; Hardinghaus and Weschke, 2022, 2023; Łukawska et al., 2023; Reckermann et al., 2024). Other factors are considered in five publications or fewer each. It is notable that while modeling travel time takes center stage in many predictive models from Section 1.1, it is of little concern for inductive models in this subsection. We believe this is primarily because observed data are more readily available and easier to handle in VoD space, since speed differs between cyclists and even high-quality GPS tracks do not always allow for precise travel time calculations for individual links.

1.3. Contributions

Summarizing the current state of research, there is clearly sustained interest in evaluating the benefits of bicycle infrastructure expansion, with transport models and in particular the software PTV Visum being established research tools. From inductive modeling, there is a solid knowledge base on factors that should be included in route choice impedance and their VoD.

However, several research gaps among transport model application studies are evident: Hebenstreit (Hebenstreit, 2021) is the only one to account for bicycle availability, albeit with static ownership rates based on survey data and no dynamic choice model. Furthermore, differences in preference regarding bicycle mode choice between person groups are not considered, and only two transport models consider differences between person groups at all, namely through different speeds (Hallberg et al., 2021; Hebenstreit, 2021). Inductive models reveal great differences between c-bikes and e-bike impedance, but most predictive transport models neglect these distinctions within cycling (Dane et al., 2020; Hardinghaus and Weschke, 2023; Meister et al., 2023; Khavarian et al., 2024). While two publications consider variations in speed between bicycle types, neither treats c-bikes and e-bikes as distinct alternatives in mode choice (Hallberg et al., 2021; Hebenstreit, 2021). As e-bike adoption rises, this omission compromises model accuracy and limits the ability to assess e-bike-specific policies. No transport model described in the literature differentiates between c-bikes and e-bikes throughout all relevant sub-models and accounts for differences between person groups. Lastly, no study known to us compares model quality before and after differentiating between c-bikes and e-bikes.

In presenting, validating, and applying such a novel model, we contribute to the literature in several ways:

- We present the first macroscopic travel demand model that dynamically differentiates between electric and conventional bicycle traffic across all sub-models and accounts for differences in preferences between the two, thereby establishing a groundwork for future researchers and practitioners and highlighting data needs and challenges in model formulation (Sections 2 and 3).
- We are the first to systematically evaluate the impact of differentiating c-bike and e-bike modeling on overall model quality by comparing several quality measures between our differentiated model and a simplified version (Section 4.1).
- We reveal the impact of policies aiming to promote cycling by evaluating three scenarios related to infrastructure expansion and e-bike ownership, thereby also demonstrating the usefulness of a differentiated modeling approach (Sections 3.6 and 4.2).

We close with discussions on the policies' impacts (Section 5.1), learnings for modeling bicycle traffic (Section 5.2), limitations (Section 5.3), and a conclusion (Section 5.4).

2. Background and data

Wuppertal, Germany, presents a challenging environment for cycling due to its steep topography and limited infrastructure. The city developed along the narrow valley of the Wupper River, with many key destinations on surrounding slopes. For example, reaching the main university campus from the city center requires covering a distance of only 2 km but gaining 100 m in elevation. Cycling infrastructure is sparse, except for the Nordbahntrasse, an east-to-west rail-to-trail corridor through the northern parts of the city. Wuppertal thus presents an ideal case study for e-bike modeling; if ineffective here, it is likely even less relevant in flatter cities, where e-bikes offer less advantage over c-bikes.

Table 2
Literature on inductive bicycle route choice modeling.

Source	E-bikes	Model type	Significant variables
Broach et al. (2012)	no	PSL	Distance, infrastructure, turns, traffic signals, commute, car volume, speed limit
Prato et al. (2018)	no	Mixed PSL	Distance, infrastructure, against one-way, turns, elevation gain, surface, vehicle lanes, land use
Dane et al. (2020)	yes	Mixed PSL	Distance, age, weekday, peak hour, daylight, endpoint at work
Huber et al. (2021)	no	MNL	Distance, infrastructure, gradient, surface, speed limit
Koch and Dugundji (2021)	no	MNL, recursive Logit	Distance, traffic signals, noise exposure, land use, water, trees, tramline, infrastructure
Scott et al. (2021)	no	PSL	Distance, directness, turns, distance between intersections, length longest leg, gradient, infrastructure
Shah and Cherry (2021)	no	PSL	Distance, infrastructure, turns, speed limit, against one-way, car volume, traffic signals, crashes, peak hour, weekend, registered user
Cho and Shin (2022)	no	PSL	Distance, intersections, traffic signals, infrastructure, gradient
de Jong et al. (2023)	no	Linear model	Distance, land use, speed limit, infrastructure, gradient
Hardinghaus and Weschke (2022)	no	MNL	Travel time, infrastructure, speed limit, surface, parking, trees
Hardinghaus and Weschke (2023)	yes	MNL	Like Hardinghaus and Weschke (2022)
Łukawska et al. (2023)	no	PSL	Distance, gradient, infrastructure, intersections, land use, against one-way, surface
Meister et al. (2023)	yes	PSL and mixed PSL	Distance, infrastructure, speed limit, traffic signals, gradient
Rupi et al. (2023)	no	Oaxaca-Blinder decomposition	Distance, gender, city center, infrastructure, directness, intersections, intersection complexity, turns
Chung et al. (2024)	no	PSL	Distance, infrastructure, land use, peak hour, crosswalks, vehicle lanes, floating population, amenities, public transport stations
Khavarian et al. (2024)	yes	MNL	Distance, street type, infrastructure, car volume, traffic signals, hills, gender
Meister et al. (2024)	no	PSL, recursive Logit	Distance, infrastructure, speed limit, traffic signals, gradient, u-turn
Reckermann et al. (2024)	no	Mixed Logit	Travel time, distance, gender, urbanity, access/egress time, cost, age, income, mandatory trip, street type, infrastructure, age, surface

For route choice calibration and validation, we used bicycle traffic volume count data provided by the City of Wuppertal (13 locations) and from earlier teaching exercises (four locations). From all counting locations potentially available to us, we only excluded two due to counting taking place on a holiday or Sunday. The count data includes intersection and cross-section sites. Directional counts are aggregated. The counting periods range from short manual counts spanning only a few hours to automated counts spanning several months. To standardize the data, we convert all counts to uniform average weekday traffic (AWT) values in a multi-step process. First, short-term counts are extrapolated to a full week using the average weekly bicycle traffic flow curve at 15 min intervals, derived from counting location 13's 2023 and 2024 records (see Fig. 1). For example, if a manual count covered only 1 PM–1:15 PM on a Wednesday, its count value is divided by 0.002267 to estimate the full week's traffic. Since all counts cover longer time spans, the corresponding interval shares are summed, and the total count is divided by this value. This approach assumes that the weekly flow curve remains consistent throughout the year. To extrapolate from weekly to yearly values (i.e. account for seasonality), data from counting location 13 cannot be used, as it does not cover all months. Instead, we rely on monthly aggregate data from 2022 to 2024 from 14 permanent counting locations in the neighboring city of Düsseldorf (Düsseldorf, 2025), which has a comparable climate. This flow curve is also shown in Fig. 1. Finally, to convert yearly traffic to AWT, we apply a factor of 0.00314906. This factor is derived from data collected at 30 counting locations in Berlin (Senatsverwaltung für Mobilität, Verkehr, Klimaschutz und Umwelt, 2024), because unlike the other two datasets, this one provides both full-year coverage and daily resolution. Fig. 2 shows the counting locations. Their original count time and the extrapolated AWT values can be found in Table A.10 in Appendix A.

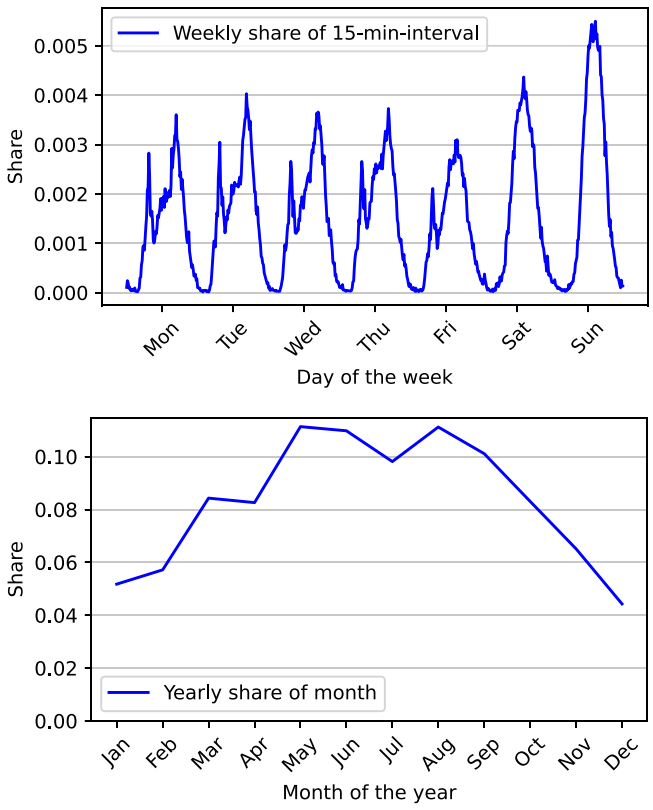

Fig. 1. Weekly flow curve in 15 min intervals from counting location 13 (top) and yearly flow curve in monthly intervals from counting locations in Düsseldorf (Düsseldorf, 2025) (bottom) used for expansion of short-term counts to AWT.

For calibrating ownership and mode choice, we use data from a mobility survey conducted in September 2020 (Stadt Wuppertal, 2021), the raw data of which are provided to us by the City of Wuppertal. Most likely due to the Covid-19 pandemic, the total cycling mode share in that survey is higher (8%) than suggested both by the previous 2011 mobility survey and by the more recent counting data (approximately 2% in each case, see Section 3.5). Therefore, after a preliminary mode and route choice calibration, we reduce target mode shares across trip purposes and person groups by a factor in such a way that the total modeled and observed bicycle traffic counts match. Figs. 3 and 4 depict these target cycling mode shares and the cycling distance distributions for Wuppertal-internal travel. For inbound travelers and children under the age of 6, no data is available.

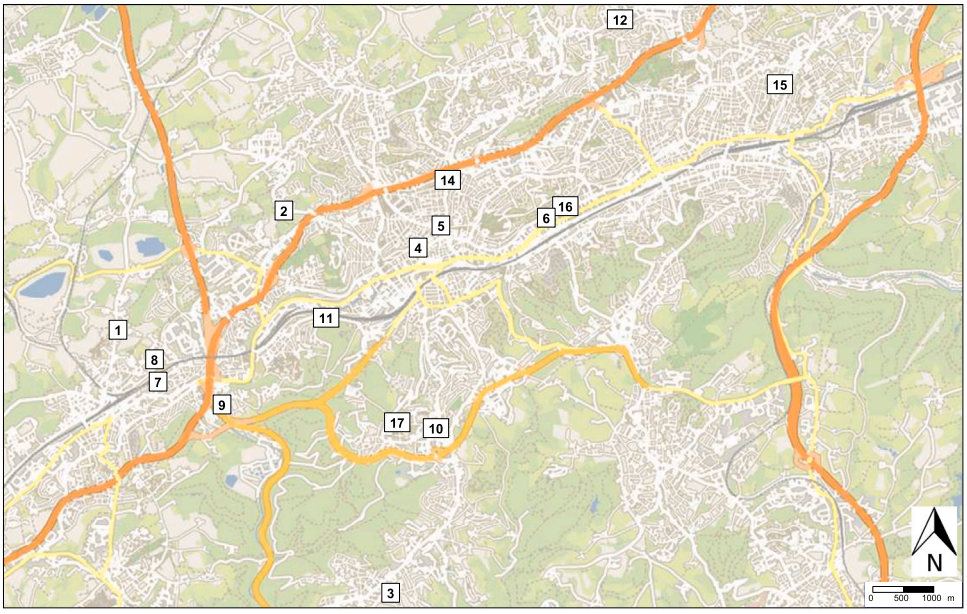

Fig. 2. Counting locations in Wuppertal. Backgroundmap © OpenStreetMap contributors, CC-BY-SA.

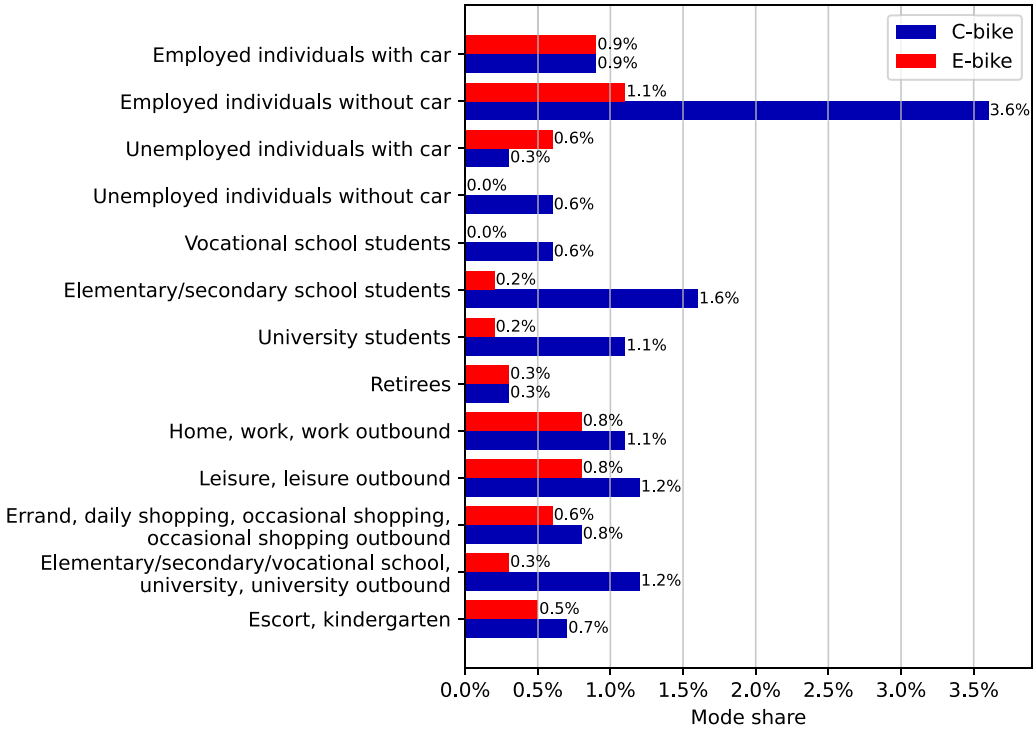

Fig. 3. Target c-bike and e-bike mode shares by person groups and trip purposes.

3. Model and scenarios

We build on an existing, calibrated PTV Visum model provided by the City of Wuppertal (Verkehrsmodell der Stadt Wuppertal, *base model*) which differentiates between car as driver, car as passenger, public transport, walking, and cycling, however, the latter two are not calibrated or assigned to the network. It represents an average weekday. In the following subsections, we describe our method to implement and calibrate c-bike and e-bike throughout all sub-models (*differentiated model*). For comparison, we also develop an equivalent *simplified model* that treats cycling as a single mode of transport. Both models are calibrated using the same procedures and data to allow for insight into whether a differentiated modeling of bicycle traffic impacts model quality. Fig. 5 shows the structure of the model.

3.1. Network model and bicycle impedance

The network model remains unchanged for car and public transport compared to the base model. There are 89 link types that represent combinations of permitted transport modes, number of lanes, maximum speed, and capacity. For example, they differentiate between a four-lane motorway with a 120 km/h speed limit and a single-lane residential road with a 30 km/h speed limit. Capacity-restraint functions are applied to account for congestion effects by increasing car

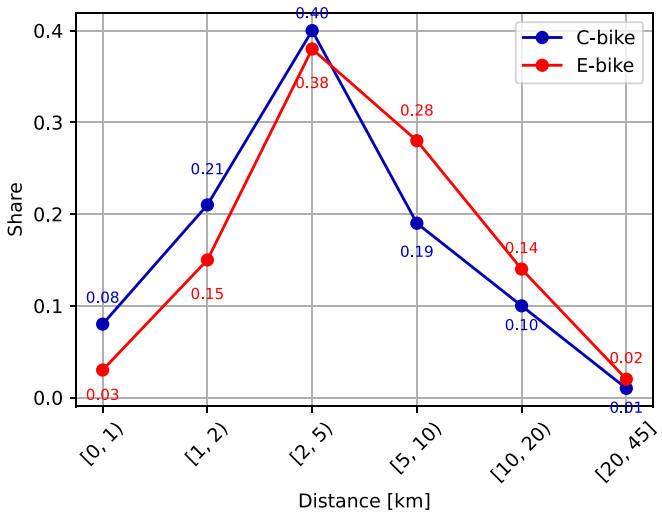

Fig. 4. Target c-bike and e-bike trip distance distributions.

travel time as capacity utilization increases. For public transport, the model uses the actual schedule of the local public transport system on a normal weekday. The study area is subdivided into 572 traffic zones, which serve as the basis for demand modeling and the computation of indicator matrices.

To represent bicycle infrastructure, we introduce the link attribute bicycle infrastructure, which can take the values: none, stairs, pedestrian zone, forest/service road, bicycle lane, bicycle path, bicycle road, or rail-trail (specifically the Nordbahntrasse). Stairs are generally blocked and one-way streets are made accessible for bicycles in both directions to reflect actual usage. Fig. 10 shows a graph of the bicycle infrastructure network. No capacity-restraint functions are applied to bicycle traffic. Elevation is written to each node using a digital terrain model (Bezirksregierung Köln, 2025), allowing the computation of a directional link attribute *gradient*. Fig. 6 illustrates the city's challenging topography.

C-bike and e-bike impedance are indicator matrices in VoD space, each containing values for all OD pairs. They are used in destination, mode, and route choice. VoD is chosen for its readily available empirical parameters (see Section 1.2) and avoids distinguishing between objective and subjective influences on travel time. When calculating the impedance for an OD pair, the route with the lowest impedance is considered.

Based on Section 1.2, we consider distance, bicycle infrastructure, turns, gradient, and motor vehicle speed limit in the two impedance functions. For bicycle type b, the impedance I of a route r consisting of links L and turns T is

$$I_{r,b} = \sum_{l \in L} dist_l * (1 + f_{infra,l} + f_{gradient,l,b} + f_{vmax,l}) + \sum_{t \in T} \theta_t, \quad (1)$$

where $dist_l$ is the length of each link, f_{infra}, $f_{gradient}$, and f_{vmax} are factors reducing or increasing each link's impedance in VoD space, and θ_t is a penalty for some types of turns. In the following paragraphs, we explain how we arrived at the VoD values for our model.

Some sources (Meister et al., 2023; Arning and Kaths, 2025a) find e-bikes to be less sensitive to **infrastructure** provision than c-bikes, while others (Hardinghaus and Weschke, 2023) find the opposite. Similarly, there is no conclusive insight into whether there is a difference between c-bikes and e-bikes regarding motor vehicle speed in mixed traffic or turns at intersections. For this reason, only the impact of gradient is differentiated by bicycle type. Table 3 reports VoD values extracted from the literature for different types of bicycle infrastructure. Sources where VoD was not explicitly reported are marked with * and the values presented are estimates based on reported parameter values and

Table 3
Literature VoD values for bicycle infrastructure.

Source	Bic. path	Bic. lane	Bic. track	Other
Broach et al. (2012)	−0.16			−0.11 (Bicycle boulevard)
Prato et al. (2018)	−0.20			2.17 (Foot path)
Huber et al. (2021)*		−1.12	−0.92	
Cho and Shin (2022)*		−1.32		
Łukawska et al. (2023)		−0.06	−0.11	−0.13 (Cycle-superhighway)
Meister et al. (2023) (c-bike)	−0.23	−1.00		
Meister et al. (2023) (e-bike)	−0.12	−1.12		

Table 4
VoD values for bicycle infrastructure used in the model.

Bicycle infrastructure	Initial f_{infra}	Final f_{infra}
Rail-trail	−0.50	−0.60
Bicycle road	−0.50	−0.50
Forest/service road, bicycle lane, bicycle path	−0.35	−0.35
Pedestrian zone, stairs, none	0.00	0.00

Table 5
Literature VoD values for a motor vehicle speed limit of 30 km/h compared to 50 km/h.

Source	VoD
Huber et al. (2021)*	−0.043
Hardinghaus and Weschke (2022)*	−0.062
Meister et al. (2023)	−0.16
Meister et al. (2024)	−0.09, −0.12, −0.14

average trip lengths. We normalize against riding in mixed traffic. The values vary strongly, from one source indicating that riding 1000 m on a bicycle lane is still equivalent to riding 937 m in mixed traffic (Łukawska et al., 2023) to other sources that find infrastructure to more than completely outweigh the objective link distance (e.g., Meister et al. (2023)). As a result, we choose medium initial values for f_{infra}, as reported in Table 4. These values are later calibrated (see Section 3.5).

Four references report VoD values for link **gradient**, either for categories (Broach et al., 2012; Meister et al., 2023, 2024) or as a linear increase in VoD for every % of added gradient (Cho and Shin, 2022). Fig. 7 visualizes the wide range of values for c-bikes. It should be noted that the two extreme cases are both from the same publication in which the authors compare two different models using the same data (Meister et al., 2024). In order not to overestimate the role of e-bikes in transport modeling, we assume modest VoD values for link slope. Namely, we assume that gradients below 2%, including downhill slopes, have no impact on impedance, and that for every %-point of gradient above 2%, $f_{gradient,c-bike}$ increases by 0.25. In other words, at 6% gradient a VoD of 1 is reached, meaning cyclists would view 2 km of cycling below 2% gradient equivalent to 1 km at 6%. For e-bikes, several studies find that e-bikes are less but not unaffected by gradient (Meister et al., 2023; Khavarian et al., 2024; Arning and Kaths, 2025a). To again not overstate the relevance of differentiated e-bike modeling, we therefore assume that e-bike impedance is still affected half as strongly as c-bike, i.e. with a VoD increase of 0.125 for every %-point in gradient above 2%. During model calibration (see Section 3.5), these values are slightly increased to 0.28 and 0.14, respectively. For the simplified model, we end up with a value of 0.27 after calibration.

Cyclists dislike riding near fast-moving traffic. Table 5 presents **speed limit** VoD values from the literature. When differentiating between c-bikes and e-bikes in a Swiss study, e-bike VoD values for 30 km/h road speed limits were positive, likely due to regulatory differences: Swiss e-bikes provide assistance up to 45 km/h, whereas German e-bikes are limited to 25 km/h (Meister et al., 2023). Lacking quantitative data on preference differences between conventional and

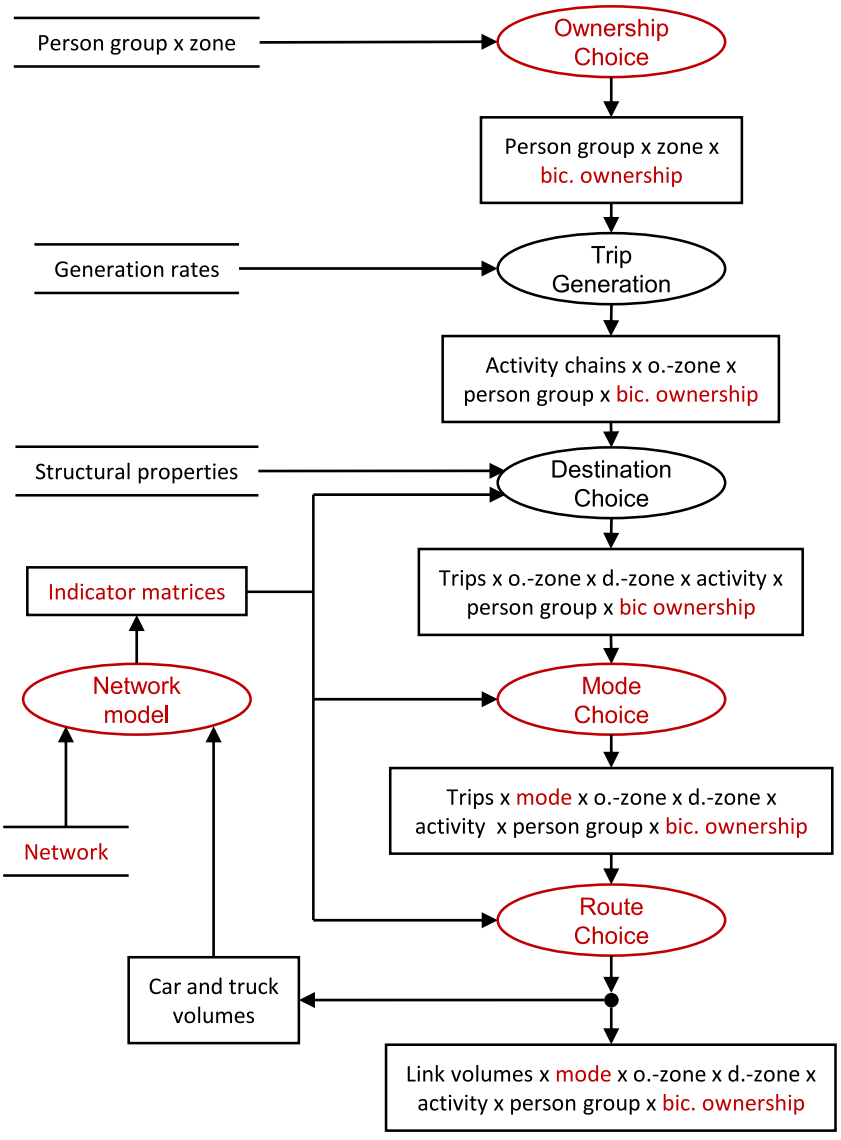

Fig. 5. Data-flow diagram of the differentiated model. Changes and additions to the base model highlighted in red. "x" separates the dimensions of demand matrices.

25 km/h e-bikes, we do not distinguish between them. Based on available VoD values, we set f_{vmax} to −0.1 for links with speed limits of 30 km/h or lower or where cyclists are unaffected by motor traffic, namely rail-trails and pedestrian zones, and 0 otherwise.

Lastly, we take into account **turns**. Due to the wide variety of intersection designs and types of turns, the VoD values reported in Table 6 are difficult to compare. For traffic signals in particular, the findings are conflicting: some sources report a high aversion of cyclists (Meister et al., 2023; Khavarian et al., 2024), some report values that are close to 0 (Łukawska et al., 2023), insignificant (Huber et al., 2021), or changing signs depending on the model used (Meister et al., 2024), and some report negative VoD values, meaning cyclists prefer routes with more signalized intersections (Shah and Cherry, 2021; Cho and Shin, 2022). For turns, values range from 22 m (Łukawska et al., 2023) to 423 m (Prato et al., 2018). In relative terms, there is little difference between c-bikes and e-bikes (Khavarian et al., 2024), prompting us to again not differentiate between the two. In light of these contradicting findings, we do not differentiate by intersection type. For left turns, we set θ to 0.05 km, close to two sources (Broach et al., 2012; Shah and Cherry, 2021) in-between more extremes values (Prato et al., 2018; Łukawska et al., 2023), and 0 otherwise.

Table 6
Literature VoD values for turns and intersections.

Source	Type of turn or intersection	VoD value [m]
Broach et al. (2012)	turn	42
Prato et al. (2018)	left turn right turn	423 221
Huber et al. (2021)*	intersection	insig.
Shah and Cherry (2021)*	left turn traffic signal	50 −33
Cho and Shin (2022)*	traffic signal intersection	−1870 740
Meister et al. (2023)	traffic signal	190
Łukawska et al. (2023)*	turn road hierarchy down turn road hierarchy up roundabout traffic signal	24 44 18 4
Khavarian et al. (2024)*	traffic signal	545

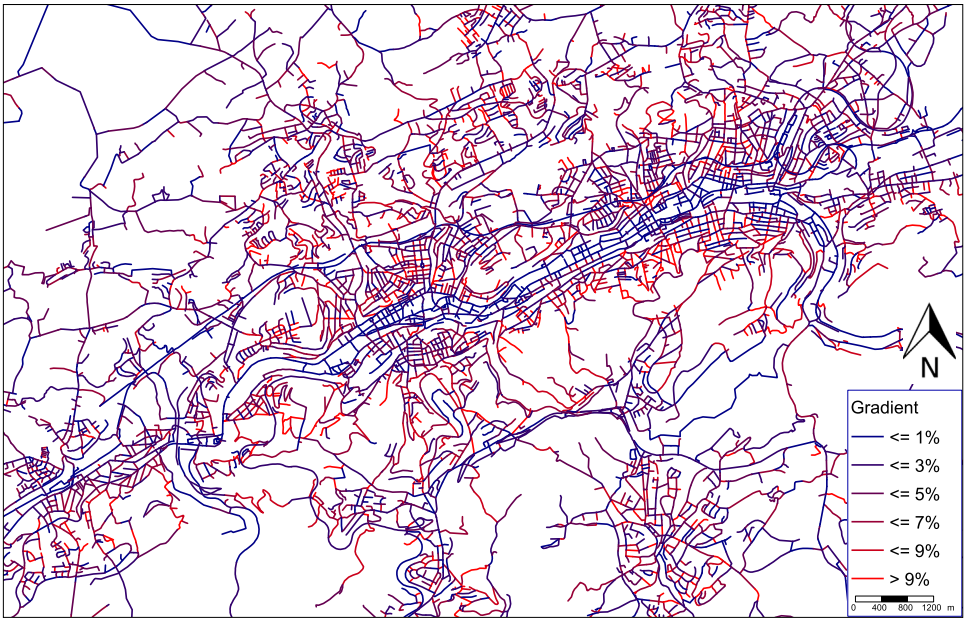

Fig. 6. Positive gradient of bicycle permissible links in the network model.

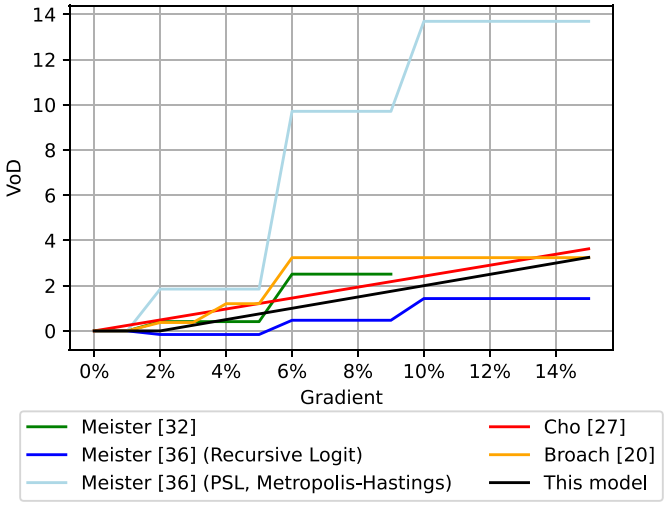

Fig. 7. VoD values for the impact of link gradient on c-bike impedance from the literature and the values chosen for the differentiated model.

Table 7
Calibrated ownership rates for model person groups.

Person group	Only c-bike	Only e-bike	Both	None
Employed individuals with car	54.1%	3.8%	14.1%	28.0%
Employed individuals without car	54.1%	3.8%	14.1%	28.0%
Unemployed individuals with car	41.2%	6.5%	16.6%	35.8%
Unemployed individuals without car	41.2%	6.5%	16.6%	35.8%
Retirees	22.9%	13.1%	25.0%	39.0%
Children	65.8%	0.0%	4.2%	30.0%
Elementary school students	65.8%	0.0%	4.2%	30.0%
Secondary school students	65.8%	0.0%	4.2%	30.0%
Vocational school students	50.1%	0.7%	3.4%	45.8%
University students	51.7%	0.5%	3.0%	44.9%
Inbound commuters	54.1%	3.8%	14.1%	28.0%
Inbound leisure travelers	54.1%	3.8%	14.1%	28.0%
Inbound shoppers	54.1%	3.8%	14.1%	28.0%
Inbound university students	50.3%	0.7%	3.6%	45.3%
Original ASC	1.75	−3.15	−1.82	0
Calibrated ASC	1.46	−2.4	−0.15	0
Total model population	46.9%	5.4%	14.7%	33.0%
Total survey population	46.9%	5.5%	14.5%	32.9%

3.2. Ownership model

C-bikes are inexpensive, so it is typically assumed in transport modeling that anyone who would regularly choose to cycle owns one. In contrast, the higher acquisition and maintenance costs of an e-bike make it essential to model ownership and mode choice separately, as many potential users do not own one. While the 2020 mobility survey includes data on c-bike and e-bike ownership, the sample size is insufficient to attain person-group-specific ownership rates. Therefore, we use an existing ownership model to model ownership rates for each person group (Arning and Kaths, 2025b). The person groups used in this model do not account for income-related differences beyond differences in mobility tool ownership and occupational status, because beyond these, income was found to have a negligible impact on e-bike use (Arning and Kaths, 2025a). We calibrate the alternative specific constants (ASC) for “only c-bike”, “only e-bike” and “both” in such a way that the share of each ownership type across the whole population matches the results of the mobility survey. The resulting ownership rates for each person group are depicted in Table 7. Across all zones, each person group is then subdivided into four subgroups, one for each ownership type. For example, our calibrated ownership model predicts that 41% of unemployed individuals with car own only a c-bike, so a zone with a population of 100 unemployed individuals with car in the base model will have 41 unemployed individuals with car and only a c-bike in the differentiated model. For the simplified model, the same approach is used. However, “only c-bike”, “only e-bike” and “both” are collapsed to “owns bicycle”. This differentiation of person group-specific and thereby also zone-level c-bike and e-bike ownership enables the model to capture spatial variation in c-bike and e-bike ownership across the urban area. As a result, it supports more detailed analyses of changes in bicycle use among population subgroups and zones than is possible with more aggregate approaches commonly found in the literature.

3.3. Trip generation and destination choice models

Trip generation and destination choice remain consistent with the base model. Visum’s VISEM procedure is used across trip generation,

destination, and mode choice. For each person group (see Table A.11 in the appendix for a complete list) and origin zone, it generates activity chains based on generation rates. For instance, a Home-Work-Errand-Home x University student generation rate of 0.0051 means that a zone with 100 university students generates 0.51 Home-Work-Errand-Home activity chains per day. Generation rates remain unchanged compared to the base model and are independent of bicycle ownership.

For destination choice, the model accounts for the relevant structural property of all potential destination zones (e.g., number of workplaces for the trip purpose work) and a cross-modal, OD-pair-specific utility. Destination choice then takes place step-wise along each activity chain for every origin zone and person group using a Logit model. The number of trips T between origin zone i and destination zone j for each step is computed as:

$$T_{ij} = O_i * \frac{S_j * exp(u_{ij})}{\sum_{j'=1}^{Z} S_{j'} * exp(u_{ij'})}, \tag{2}$$

where O denotes the number of originating trips, S the relevant structural property, and Z the number of zones. Utility is defined by

$$u_{ij} = a_{pg,purp} * ModeLogSum_{ij} + b_{pg,purp} * CarDist_{ij}. \tag{3}$$

Here, $CarDist$ is the car travel distance matrix between all zones, while $ModeLogSum$ aggregates the mode-specific mode choice utilities (see Section 3.4) in a log-sum formulation. The parameters a and b are specific to trip purpose ($purp$, see Table A.12 in the appendix for a complete list) and person group (pg) and remain unchanged compared to the base model.

3.4. Mode choice model

The mode choice utility functions for walking, car as driver, car as passenger, and public transport remain unchanged from the base model and are given in Eqs. (4), (5), (6), and (7), respectively. The term $c_{mode,pg}$ represents both person group-specific and mode-specific constants, capturing differences in mode choice preference between person groups. Indicator matrices TT, DIS, AET, RT, TF, and DWT denote travel time, distance, access/egress time, ride time, transfers, and departure waiting time, respectively.

$$u_{foot,i,j,pg} = -0.12 * TT_{foot,i,j} - 1.2 * ln(DIS_{foot,i,j}) + c_{foot,pg} \tag{4}$$

$$u_{card,i,j,pg} = -0.08 * TT_{car,i,j} - 0.12 * AET_{car,i,j} + 0.6 * ln(DIS_{car,i,j}) + c_{card,pg} \tag{5}$$

$$u_{carp,i,j,pg} = -0.08 * TT_{car,i,j} - 0.12 * AET_{car,i,j} + 0.6 * ln(DIS_{car,i,j}) + c_{carp,pg} \tag{6}$$

$$u_{pt,i,j,pg} = -0.06 * RT_{pt,i,j} - 0.09 * AET_{pt,i,j} - 1 * TF_{pt,i,j} - 0.12 * DWT_{pt,i,j} + 0.8 * ln(DIS_{pt,i,j}) + c_{pt,pg} \tag{7}$$

To introduce c-bike and e-bike, we build on findings from an existing mode choice model (Arning and Kaths, 2025a). As nesting c-bike and e-bike was rejected in that work, they are treated independently. The utility functions for c-bike and e-bike are given in Eqs. (8) and (9), respectively. Beyond the factors already captured in c-bike and e-bike impedance I (see Section 3.1), p captures person-group-specific preferences, q accounts for trip-purpose-specific preferences, and n reflects each bicycle type's distance sensitivity. In the simplified model, a single bicycle utility function of the same structure is used.

$$u_{cbike,i,j,pg,purp} = n_{cbike} * ln(I_{cbike,i,j}) + p_{cbike,pg} + q_{cbike,purp} \tag{8}$$

$$u_{ebike,i,j,pg,purp} = n_{ebike} * ln(I_{ebike,i,j}) + p_{ebike,pg} + q_{ebike,purp} \tag{9}$$

Like in destination choice, mode choice also occurs along a chain of activities for each person group and origin zone. For each trip from i to j, the share P of mode m is given by:

$$P_{ijm} = \frac{exp(u_{mij})}{\sum_{m'}^{M} exp(u_{m'ij})}. \tag{10}$$

The VISEM procedure has two important features: car, c-bike, and e-bike are not included in the choice sets of person groups without access to the respective vehicle. Consequently, car, c-bike and e-bike ownership is not considered in the utility functions. Additionally, if the first trip in a chain uses a car or bicycle, the same mode is used for the subsequent trips in the chain to bring the vehicle home. Conversely, if the first trip occurs without a car or bicycle, these modes remain unavailable. Bike and car-sharing in Wuppertal are negligible.

The two parameters n are calibrated to match c-bike and e-bike trip distance distributions (Fig. 4), while p and q are calibrated to mode shares by person group and trip purpose (Fig. 3). The model includes 56 person groups (four bicycle ownership types per person group in the base model), six modes, and 16 trip purposes, resulting in 2,280 utility functions requiring calibration. Additionally, n, p, and q must be iteratively adjusted due to their interdependent effects. Calibration was semi-automated using the Visum COM-API and Python. The code is available on GitHub (*link removed for peer review*).

To ensure comparability between the differentiated and simplified model, we define a common calibration stop-point: parameters p and q are adjusted to one decimal place of accuracy until the scalable quality value (SQV, see 4.1) of the mode share for the respective person group or trip purpose mode no longer improves. For n, the coincidence ratio (CR, see 4.1) of the observed and modeled bicycle-type-specific trip distance distribution is used. Calibrating bicycle mode choice required several hundred iterations and weeks of computation on a 3 GHz processor with 16 GB RAM. Initial values for parameter n were −1 (c-bike), −0.5 (e-bike), and −0.9 (bicycle, simplified model), with final calibrated values of −0.9, −0.4, and −0.7, respectively. Table A.13 in the appendix lists equivalent values for parameters p and q. The resulting distance distributions are presented in Section 4.1 and mode shares by person group and trip purpose in Table A.14 in the appendix. Mode shares for originating traffic are visualized spatially in Fig. 8. These are mainly influenced by local bicycle ownership and structural properties, with relation-specific mode shares more strongly influenced by gradient and bicycle infrastructure.

3.5. Route choice model

C-bike and e-bike impedance from Section 3.1 are used as the utility for c-bike and e-bike route choice, respectively. Unlike in mode choice, no distinction is made between person groups or trip purposes. For each bicycle type and OD pair, Visum's bicycle assignment procedure first identifies the route with the lowest impedance. Additional viable routes are then generated in ten iterations by randomly varying segment impedances of the original optimal route to find new routes. Routes with meshes posing a large detour to the ideal route are removed. For each OD pair ij and bicycle type b, trips T are then assigned to a specific route r among all N viable routes s using a PSL model:

$$T_{ijbr} = T_{ijb} * \frac{exp(I_{rb}) * PS_r}{\sum_{s=1}^{N} (exp(I_{sb}) * PS_s)} \tag{11}$$

This stochastic assignment accounts for random variance in cyclists' preferences. The Path-size factor PS for route r is determined by the shared length of routes r and s, $dist_{rs}$, relative to their respective total lengths $dist_r$ and $dist_s$:

$$PS_r = \frac{1}{\sum_{s=1}^{N} \frac{dist_{rs}}{\sqrt{dist_r * dist_s}}}. \tag{12}$$

As indicated by the splitting arrow below route choice in Fig. 5, the model iterates between route, destination, and mode choice because car traffic volumes influence car travel times, affecting not only route but

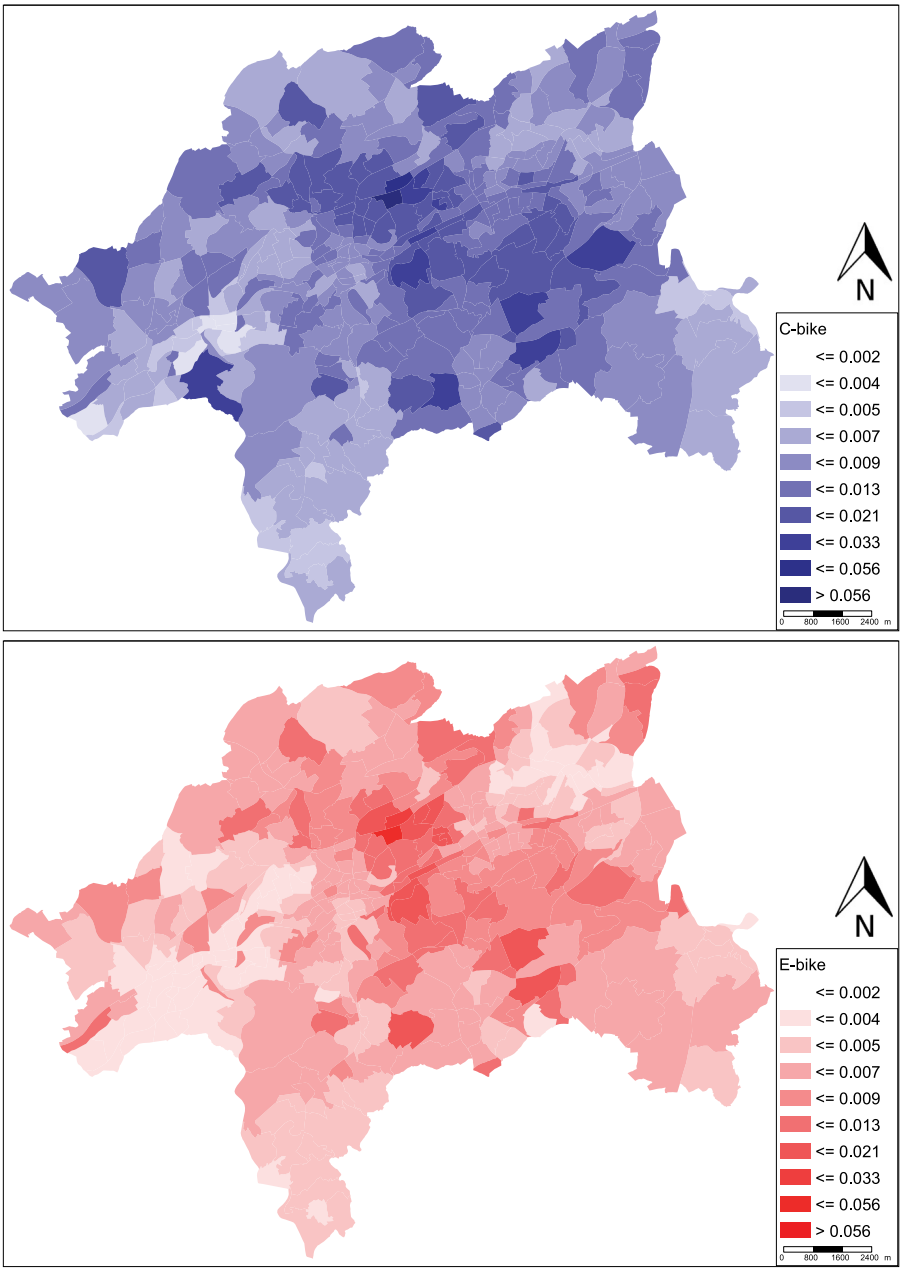

Fig. 8. C-bike (top) and e-bike (bottom) mode share among all trips originating in each zone in Wuppertal.

also destination and mode choice. Iterations continue until car traffic volume changes by fewer than 10 vehicles on every link.

C-bike and e-bike route choice was calibrated using the extrapolated count data presented in Section 2. Preliminary results showed that target mode shares from the mobility survey were unrealistically high compared to recent count data. To align total modeled bicycle counts with reality, target mode shares were scaled down by a factor of 4.34. After recalibrating mode choice accordingly, total bicycle counts matched well. Individual count deviations that remained were then addressed by calibrating the parameters of c-bike and e-bike impedance (see Section 3.1. Specifically, we adjusted the VoD factor for rail-trail from −0.5 to −0.6 and increased the gradient VoD from 0.25% and 0.125% to 0.28% and 0.14% for c-bikes and e-bikes, respectively. We also corrected some infrastructure attribution errors and added missing zone connectors. Since adjustments to impedance also affects mode choice, mode choice was calibrated a third time. This final calibration had negligible impact on route choice results, requiring no further adjustments. The same calibration procedure was applied to the simplified model. Fig. 9 shows modeled AWT bicycle traffic volumes with the Nordbahntrasse clearly visible. For observed and modeled values at counting locations before and after calibration, see Table A.18 in the appendix. During count 14, we differentiated manually between c-bikes and e-bikes. 52.8% of bicycles were identified as e-bikes on that day, confirming the general plausibility of the model's results on that link (43.5%) in that regard. Part of that difference might be due to a higher seasonality of e-bike travel compared to c-bike travel (Arning and Kaths, 2025a), resulting in counting location 14's e-bike share in May being higher than the true yearly average.

3.6. Scenarios

All scenarios build on the differentiated model, which also denotes the *Reference Scenario*, to allow for e-bike-specific interventions and analyses. For *Scenario A*, we implement all main routes envisioned in

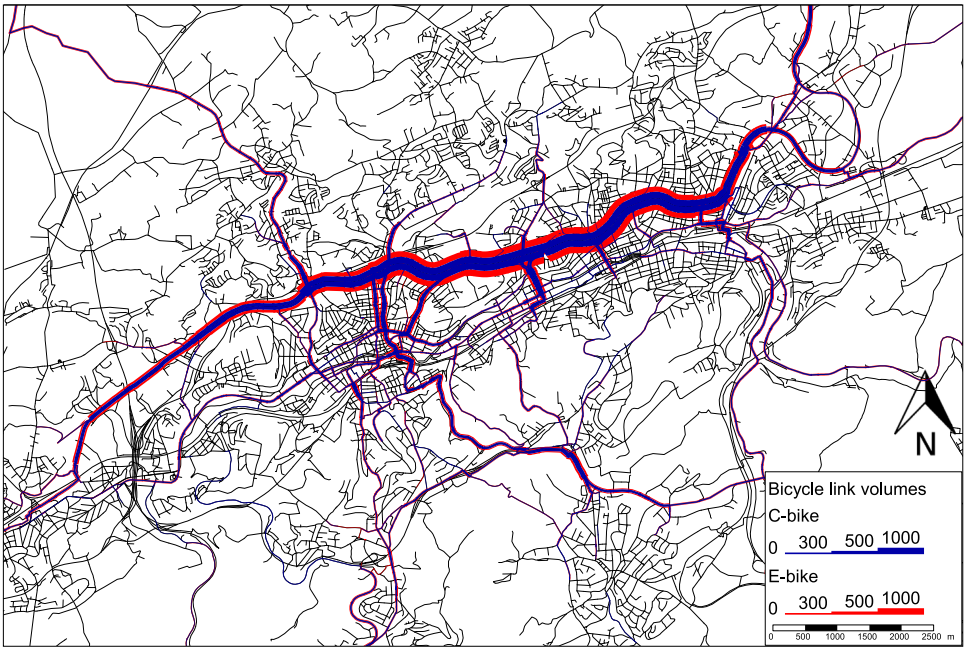

Fig. 9. C-bike and e-bike AWT in Wuppertal in the differentiated model after calibration.

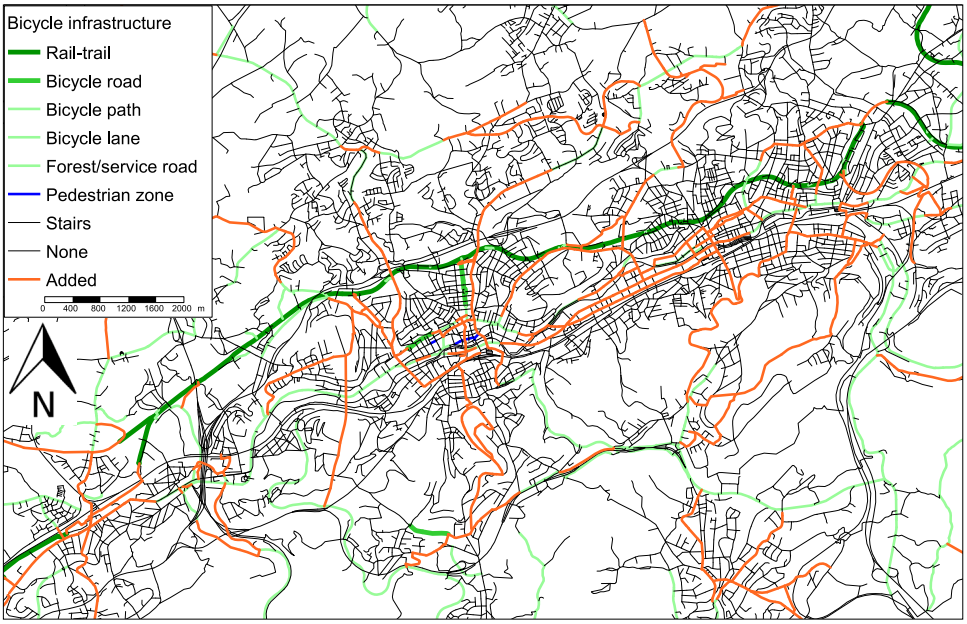

Fig. 10. Bicycle infrastructure in the Reference Scenario and sections added in Scenario A.

the 2019 Bicycle Traffic Concept of the City of Wuppertal, roughly doubling the length of both rail-trail and other bicycle infrastructure. Added segments are always coded as bicycle path or, when continuing the Nordbahntrasse, rail-trail. Fig. 10 compares the bicycle infrastructure in the Reference Scenario and Scenario A.

In *Scenario B* we model the impact of a policy, such as a purchase subsidy, doubling e-bike availability in Wuppertal. To attain new person-group-specific ownership rates, we recalibrate the ASCs from Table 7 to new total target shares of 32.3%, 10.9%, 29.1%, and 27.5% for only c-bike, only e-bike, both, and none, respectively. Lastly, in *Scenario C* we combine the changes of Scenarios A and B.

4. Results

4.1. Model quality

In this subsection, we evaluate whether the differentiated model not only enables more detailed analyses but also achieves higher quality

after calibration. Pestel (2021) differentiates two categories of quantitative quality measures: those evaluating differences between model results and reality and those assessing model behavior through realism, sensitivity, and scenario analyses. The latter category is less applicable here due to limited empirical knowledge about reasonable model behavior regarding e-bikes. For the first category, Friedrich et al. (2019) compile model results relevant for quality assessment and appropriate quality measures and thresholds.

To investigate mode choice validity, we apply the Scalable Quality Value (SQV) to average trip distance and average travel time per mode and the Coincidence Ratio (CR) to trip distance and trip travel time distributions per mode. Modeled trip-purpose and person-group-specific mode shares match the target mode shares almost perfectly in both the differentiated and the simplified model (Table A.14 in the appendix). To investigate route choice validity, we apply the SQV to bicycle AWT counts. To facilitate comparison between the differentiated and simplified models, c-bike and e-bike results are aggregated. The CR is computed according to Eq. (13), where PM_c and PO_c denote the modeled and observed shares of distance or travel time class c, using ten equiquantile classes (Pestel, 2021) based on the Wuppertal mobility survey. A CR>0.7 is deemed sufficient (Cambridge Systematics, Inc., 2010; Friedrich et al., 2019). The SQV, calculated via Eq. (14), measures deviations between modeled (M) and observed (O) values, with a scaling factor f allowing the quality measure to be applied to model results of different magnitudes. Appropriate scaling factors are 10,000 for daily bicycle counts, 5 for average travel distance, and 18 for travel time (Pestel, 2021). An SQV>0.75 is considered acceptable (Friedrich et al., 2019).

$$CR = \frac{\sum_{c=1}^{C}(min(PM_c, PO_c))}{\sum_{c=1}^{C}(max(PM_c, PO_c))} \tag{13}$$

$$SQV = \frac{1}{1 + \sqrt{\frac{(M-O)^2}{f*O}}} \tag{14}$$

The differentiated model shows a slightly better fit for average bicycle trip distance (SQV of 94% and 90%) but performs slightly worse for average travel time (84% and 86%). Note that bicycle travel time is less critical, as it was not the primary focus of the model. All other modes remain nearly unchanged. For the distributions, the differentiated model also slightly outperforms the simplified model, with CRs of 73% and 72% for bicycle trip distance and 78% and 77% for bicycle travel time. Again, other modes show even less variation. Table A.15 in the appendix presents the results in more detail. The complete distributions are provided in Tables A.16 and A.17 in the appendix. Finally, we evaluate route choice validity. Despite recalibration in the simplified model and substantial changes in traffic volumes at individual counting locations, overall bicycle route choice validity remains largely unaffected, with an average weighted SQV across all locations of 0.90 for both models. Individual counting location values are listed in Table A.18 in the appendix. In summary, validation shows that we achieved acceptable model quality for bicycle traffic and that the differentiated model is only marginally better than the simplified model.

4.2. Scenario impacts

We expect bicycle infrastructure expansion to increase c-bike and e-bike mode share and mileage, while additional e-bikes should increase e-bike usage, partially at the expense of c-bikes. The overall cycling mode shift in Scenario C may exceed the sum of A and B due to synergy or fall short due to saturation effects. Table 8 presents the model results for each scenario and the changes compared to the Reference Scenario. Synergy represents the difference between Scenario C's change and the sum of A's and B's change, e.g., $-0.006\%p = -0.14\%p - (-0.12\%p) - (-0.02\%p)$. Car modal split includes both car drivers and passengers, while mileage considers only drivers.

As expected, Scenario A increases both bicycle types' modal split and daily mileage, albeit only very modestly by 0.12%p and 7035 km, respectively. The greater increase for c-bikes suggests e-bike travel is constrained by ownership rates. Notably, while the increase in bicycle trips mostly replaces car trips (−0.07%p), total car mileage rises (4438 km). This is due to the inclusion of bicycle impedance in the log-sum term of destination choice, which increases trip lengths across all modes. In Scenario B, doubling e-bike availability roughly doubles e-bike modal share and mileage. 58% of new e-bike mileage is induced traffic. Among the replaced modes, car mileage declines the most (−13341 km), accounting for 19% of e-bike mode shift. Scenario B generates not just more mileage but also new trips: while Scenario A adds only 301 trips (+0.03%), Scenarios B and C increase trips by 2212 (+0.23%) and 2470 (+0.26%), respectively.

Scenario C combines both previous scenarios, leading to a greater increase in cycling. Synergy effects show that the combined impact on bicycle modal share and mileage closely matches the sum of the individual scenarios, differing by only 0.006%p and −77 km, respectively. When differentiating between bicycle types, however, it is revealed that the two measures in combination lead to a stronger decrease in c-bike travel and increase in e-bike travel than if the two measures are evaluated separately. Additionally, public transport substitution is more pronounced when both measures are implemented together.

Beyond mode shift, we examine bicycle impedance reduction as a key benefit of infrastructure expansion. While travel time savings are typically prioritized in analysis (e.g., Hallberg et al. (2021), Rich et al. (2021), Argyros et al. (2024)), our model operates in VoD rather than VoT space and does not explicitly model speed. However, our approach allows to quantify the improvement of "soft" factors beyond speed. We first compute total encountered c-bike and e-bike impedance across all trips in the Reference Scenario and then recalculate using the same trip matrices but Scenario A's impedance matrices. To account for partial impedance reductions for new bicycle trips, we apply the Rule of Half, assuming each added trip benefits from half the average impedance reduction of Reference Scenario trips. Table 9 presents our results: Scenario A reduces total impedance by 12,257 km per day. Monetizing this reduction in VoD space is less straightforward than for travel time, as e.g. willingness-to-pay values are not readily available. We can, however, make some analogies to visualize its magnitude: cautiously assuming a value of time of 10€/h and an average speed of 15 km/h yields a daily benefit of 8171€ or nearly 3 million€ annually.

5. Discussion and conclusion

5.1. Impacts of bicycle ownership and infrastructure on cycling

Promoting active mobility while reducing car dependency is key to livable cities. Our model confirms that expanding bicycle infrastructure increases cycling, although the mode shift may be smaller than expected given the ambition of the modeled network additions. This aligns with other studies on large-scale infrastructure expansion (Hallberg et al., 2021; Oskarbski et al., 2021; Liu et al., 2021), although some report stronger increases (Rich et al., 2021; Paulsen and Rich, 2024). Our differentiated modeling approach reveals that infrastructure expansion primarily boosts c-bike mode share, as low e-bike ownership limits e-bike use. In contrast, promoting e-bike ownership drastically increases e-bike use, with the car being the most strongly substituted mode after induced travel–an important factor for assessing environmental impact. This finding aligns with meta-analyses on e-bike substitution rates (Bigazzi and Wong, 2020; Bourne et al., 2020).

Our findings show negligible synergies between Scenarios A and B in terms of modal split and mileage. We conclude that the combined impact of infrastructure expansion and e-bike promotion depends on the nature of the improvements. If infrastructure expansion mainly reduces gradients, such as the added bridge part of our Scenario A, additional benefits from increased e-bike adoption are likely smaller. However, if

Table 8
Relevant scenario results and relative change compared to the reference scenario.

Indicator	Mode	Reference	A	Change	B	Change	C	Change	Synergy
Modal split	walk	20.50%	20.49%	−0.02%p	20.39%	−0.12%p	20.36%	−0.14%p	−0.006%p
	c-bike	1.14%	1.23%	0.09%p	1.09%	−0.05%p	1.17%	0.03%p	−0.012%p
	e-bike	0.77%	0.79%	0.02%p	1.53%	0.76%p	1.57%	0.80%p	0.018%p
	c-bike+e-bike	1.91%	2.02%	0.12%p	2.62%	0.71%p	2.74%	0.84%p	0.006%p
	car	58.36%	58.28%	−0.07%p	57.96%	−0.39%p	57.91%	−0.45%p	0.015%p
	public transport	19.23%	19.21%	−0.03%p	19.03%	−0.20%p	18.99%	−0.24%p	−0.015%p
Mileage [km]	walk	205 280	205 076	−204	204 098	−1182	203 783	−1497	−111
	c-bike	79 630	84 988	5359	76 391	−3239	80 620	991	−1129
	e-bike	69 887	71 564	1677	139 820	69 933	142 549	72 662	1052
	c-bike+e-bike	149 516	156 552	7035	216 210	66 694	223 169	73 653	−77
	car	2 389 371	2 393 810	4438	2 376 031	−13341	2 380 900	−8471	431
	public transport	1 312 280	1 311 608	−671	1 300 699	−11580	1 298 739	−13540	−1289

Table 9
Impedance reduction due to infrastructure expansion.

	C-bike	E-bike
Trips reference	10 830	7301
Impedance reference [km]	91 479	72 490
Impedance A [km]	84 776	67 289
Diff. A-reference [km]	−6704	−5201
New trips	876	228
Diff. A-Reference rule of half [km]	−271	−81
Total impedance reduction [km]	−6975	−5282

the infrastructure is designed to minimize riding in mixed traffic, which both c-bikes and e-bikes profit off equally, positive synergies can be expected.

While we do not explicitly quantify travel time savings, which have been identified in previous studies as a key benefit of infrastructure expansion (Liu et al., 2021; Oskarbski et al., 2021; Hallberg et al., 2021; Rich et al., 2021; Paulsen and Rich, 2024; Argyros et al., 2024), our model allows quantifying the change in the overall attractiveness of cycling, incorporating distance, infrastructure, gradient, motor vehicle speed, and turns within VoD space. By quantifying this impedance reduction for both existing and new trips, we show that infrastructure expansion not only increases cycling, but also considerably improves conditions for current cyclists, highlighting broader benefits beyond travel time savings. These additional benefits should be considered in infrastructure appraisal, with further work needed to appropriately monetize them.

5.2. Modeling electric bicycle traffic

Differentiating c-bikes from e-bikes enables analyzing e-bike-specific policies, measures, and impacts. However, it did not meaningfully improve model quality, even when focusing on the validity of cycling-related model results and despite high shares of e-bike travel among cycling and hilly terrain in our case study. This suggests that unless the focus is on e-bike-related policies or model results, treating bicycle traffic as a uniform mode remains a valid and efficient approach.

For cities aiming to use e-bike-specific transport models to guide decisions on sustainable mobility, infrastructure planning, and policy development, several recommendations can be made. First, collecting detailed travel behavior and ownership data, segmented by bicycle type and user demographics, is crucial for accurately modeling c-bike and e-bike usage. Given the relatively uniform distribution of e-bike use across the network and a low relevance of link-specific e-bike shares for infrastructure design, unsegmented bicycle count data are sufficient, even for assessments in very hilly contexts like ours. However, this may be inadequate in contexts involving higher-speed e-bikes, such as in Switzerland or other regulatory environments.

From a mathematical perspective, VoT and VoD impedance are interchangeable–all factors can be included in either formulation, and parameters can be transformed from VoD to VoT space and reverse. Because travel time, unlike distance, is objectively affected by factors such as gradient or infrastructure, VoT space has so far been preferred in other modeling studies. This introduces challenges, as some factors affect objective travel time (e.g., bicycle speed limits), some need to be included even though they do not affect objective travel time (e.g., motor vehicle speed), and some impact both (e.g., infrastructure). These complexities make it difficult to separate objective and subjective effects in impedance formulation and to gather appropriate VoT values. The VoD approach, on the other hand, is simpler to implement, as all factors can be treated as fully subjective in relation to travel distance. If travel time savings are of analytical concern, more sophisticated speed modeling is required. This does not mean the model itself must operate in VoT space: Travel time can be computed solely as an indicator matrix for impact analysis, while impedance still operates in VoD space. In this case, it is crucial to consider that improving bicycle conditions (e.g., adding infrastructure) may increase travel time (e.g., due to cyclists taking detours). The subjective improvements captured in the VoD impedance should then also be included in the policy appraisal.

5.3. Limitations

Several limitations apply to the interpretations of our scenario impacts. The ownership model does not account for infrastructure expansion increasing bicycle ownership, thus slightly underestimating additional bicycle travel in Scenario A. New e-bike owners would likely use their e-bikes less than early adopters, leading to an overestimation of additional e-bike travel in Scenario B. Lastly, since c-bike and e-bike mode choice utilities are included in the log-sum terms of destination choice despite their low overall share, induced mileage from improved bicycle accessibility is likely overstated.

Further limitations apply to our model in general. While the expansion of bicycle count data to AWT accounted for daily, weekly, and seasonal variations, it did not consider weather or dominant trip purposes at each location. In some cases, only a few hours were counted. Thus, comparing route choice validity between the differentiated and simplified model might not be limited by model quality but by consistency between counting locations. Similarly, adjusting 2020 travel survey data to match observed count volumes may skew person-group-specific target mode shares, as some groups, such as former public transport commuters, likely increased their cycling more during the COVID pandemic than others, such as schoolchildren who already cycled to school at considerable rates before the pandemic. Although Wuppertal provides a strong example for e-bike modeling, further case studies are needed to confirm the impact of differentiated modeling on model quality, especially in areas with higher levels of cycling and better data.

Some limitations of our model stem from its macroscopic nature. In contrast, agent-based approaches (Kaziyeva et al., 2021; Hebenstreit, 2021; Jafari et al., 2022) enable a more disaggregated and behaviorally rich representation of individual travelers and their activity patterns. For instance, intra-household dynamics, such as the constraint that a single e-bike in a two-person household cannot be used by both members simultaneously, cannot be represented in our modeling framework. Similarly, adaptive changes in individuals' activity schedules in response to the availability of new mobility options cannot be captured.

Lastly, and most importantly, our model does not capture the effects of cultural change: bicycle traffic is not only influenced by factors such as infrastructure, travel time, or gradient. Local mobility cultures can lead to significant differences in bicycle use between places and times with otherwise similar characteristics. Improving bicycle infrastructure may signal to the city society that cycling is desirable, especially when paired with soft measures like campaigns. Additionally, there is evidence that increased bicycle traffic can in turn lead to even more cycling through normalization (den Hoed, 2025) and safety in numbers effects (Elvik and Goel, 2019). Future research should incorporate these societal dynamics into transport models to more accurately assess the impact of policies promoting active mobility.

5.4. Conclusion

We developed the first macroscopic transport model that dynamically differentiates between electric and conventional bicycle traffic across all sub-models, demonstrating its analytical advantages over traditional approaches. Our study revealed that while bicycle infrastructure expansion increases cycling, improvements for existing bicycle travel beyond mere travel time benefits are of high relevance. To promote e-bike use, increasing e-bike availability is key. Most of the new e-bike travel is induced or replaces car usage, highlighting e-bikes' potential to not just replace other active modes or public transport, but reduce car dependence and greenhouse gas emissions. Synergies between infrastructure expansion and e-bike ownership promotion were negligible in our case study.

For cities evaluating e-bike-specific measures or impacts, such as e-bike subsidies or electric and conventional cycling rates, differentiating between the two types of bicycles in transport modeling is essential. This requires sufficient data on c-bike and e-bike ownership and use as well as bicycle count data, which can be a practical challenge. We recommend using route choice bicycle impedance as the foundation for mode and destination choice, with additional factors considered in the latter sub-models where relevant. While both value of distance and value of time formulations are feasible, we suggest using value of distance due to easier availability of appropriate parameter values and simpler impedance formulation. If accurate travel time is of interest for analysis, it can be computed as an additional model output. While offering more analytical possibilities, the differentiated modeling approach did not improve model quality, even though our study area is very hilly. For use cases not specifically focused on e-bike traffic, undifferentiated bicycle modeling therefore remains an effective solution.

The electrification of bicycle traffic is a revolution of active mobility–and it is ongoing. To integrate e-bikes into smart, clean, and healthy transportation systems, cities have to truthfully represent this revolution in their transport models and policy evaluations.

CRediT authorship contribution statement

Leonard Arning: Writing – review & editing, Writing – original draft, Visualization, Validation, Software, Resources, Project administration, Methodology, Investigation, Formal analysis, Data curation, Conceptualization. **Heather Kaths:** Writing – review & editing, Supervision, Resources, Project administration, Funding acquisition.

Declaration of Generative AI and AI-assisted technologies in the writing process

During the preparation of this work the authors used ChatGPT-4 in order to revise language, grammar, spelling, and punctuation. After using this tool/service, the authors reviewed and edited the content as needed and take full responsibility for the content of the publication.

Declaration of competing interest

The authors declare that they have no known competing financial interests or personal relationships that could have appeared to influence the work reported in this paper.

Appendix A

See Tables A.10–A.18.

Table A.10
Counting locations and extrapolated average weekday traffic (AWT) values.

Nr.	Location	Source	Original counting period	AWT
1	Bahnstr.	City	Tue, May 23, 2023, 8:30–9:30 and 15:30–16:30	236
2	In der Beek	City	Thu, Aug 29, 2024, 7:00–9:00 and 15:00–17:00	439
3	Sambatrasse	City	Tue, Mar 15, 2022, 7:15–8:45 and 15:00–17:00	238
4	Luisenstr.	City	Tue, Sep 3, 2024, 7:00–8:45 and 15:15–17:00	882
5	Karlstr./Friedrich-str.	Own	Wed, May 17, 2023, 7:00–18:00	974
6	Völklinger Str./Hünefeldstr.	Own	Tue, May 23, 2023, 7:00–18:00	509
7	Herderstr.	City	Wed, Mar 22, 2023, 7:00–9:00 and 15:00–17:00	868
8	Homanndamm	City	Thu, Aug 24, 2023, 7:00–8:30 and 15:00–17:30	1439
9	Rutenbeck	City	Wed, Mar 3, 2021, 6:45–8:15 and 14:30–16:30	234
10	Jung-Stilling-Weg/East	City	Wed, Aug 28, 2024, 7:30–10:30 and 15:00–17:00	295
11	Schwarzer Weg	City	Thu, Sep 23, 2021, 7:00–9:00 and 15:30–17:30	106
12	Hatzfelder Str.	City	Thu, May 25, 2023, 8:00–10:00 and 14:00–16:00	159
13	NBT/Wüstenhofer	Own	June–August 2023, February–June 2024	2150
14	NBT/Uellendahler	Own	Tue, May 14, 2024, 7:00–13:00	3191
15	Luhnstr.	City	Thu, Nov 3, 2022, 8:30–9:00 and 16:00–16:30	1187
16	Hünefeldstr.	City	Wed, Sep 29, 2021, 7:00–9:00 and 15:00–17:00	385
17	Jung-Stilling-Weg/West	City	Wed, Aug 28, 2024, 7:30–10:30 and 12:30–14:30	722

Table A.11
Person group abbreviations.

Person group	Abbreviation
Employed individuals with car	EMPwC
Employed individuals without car	EMPwoC
Unemployed individuals with car	UEMPwC
Unemployed individuals without car	UEMPwoC
Retirees (age 65 and above)	Retirees
Children	Child
Elementary school students	ElemStud
Secondary school students	SecStud
Vocational school students	VocStud
University students	UniStud
Inbound commuters	InbW
Inbound leisure travelers	InbL
Inbound shoppers	InbB
Inbound university students	InbU

Table A.12
Trip purpose abbreviations.

Trip purpose	Abbreviation
Home	H
Work	W
Leisure	L
Errands	E
Shopping daily needs	S
Shopping occasional needs	B
Elementary school	Se
Secondary school	Ss
Vocational school	Sv
University	U
Escort	C
Kindergarten	K
Outbound work	Wx
Outbound leisure	Lx
Outbound shopping	Bx
Outbound university	Ux

Table A.13
Values for bicycle mode choice parameter p (person groups) and q (trip purposes) before and after calibration.

Person group, trip purpose	C-bike		E-bike		Bicycle	
	Initial	Final	Initial	Final	Initial	Final
EMPwC	0	1.9	0	−0.9	3.2	2.6
EmpwoC	0	2.6	0	−1.6	3.9	2.8
UEMPwC	0	0.9	0	−1.9	2.3	1.9
UEMPwoC	0	0.9	0	−15.0	2.1	0.6
VocStud	2	1.1	0	−25.0	2.5	1.2
ElemStud, SecStud	4	1.9	−4	−2.0	3.2	2.1
UnivStud	4	2.2	−2	−1.0	3.8	2.5
Retirees	−2	1.0	4	−3.1	2.8	1.8
Child	2	3.9	−4	−35.0	5.0	3.5
InbW, InbL, InbB, InbU	0	3.7	0	0.1	5.0	4.1
W, Wx, H	0	0.1	0	0.2	0.7	0.5
L, Lx	1	0.2	1	0.4	0.7	0.6
E, S, B, Bx	−4	−0.1	−2	0.3	0.2	0.2
Se, Sv, Ss, U, Ux	1	0.2	−6	0.7	0.7	0.5
C, K	−6	−0.9	−2	0	−0.5	−0.3

Table A.14
Mode shares by person group and trip purpose in the observed data and the calibrated differentiated and simplified model.

Person group, trip purpose	Observed			Diff. model			Simp. model
	c-bike	e-bike	bicycle	c-bike	e-bike	bicycle	bicycle
EMPwC	0.9%	0.9%	1.8%	0.9%	0.9%	1.8%	1.8%
EMPwoC	3.6%	1.1%	4.7%	3.5%	1.1%	4.6%	4.7%
UEMPwC	0.3%	0.6%	0.9%	0.3%	0.5%	0.8%	0.9%
UEMPwoC	0.6%	0.0%	0.6%	0.6%	0.0%	0.6%	0.6%
VocStud	0.6%	0.0%	0.6%	0.5%	0.0%	0.5%	0.6%
ElemStud, SecStud	1.6%	0.2%	1.8%	1.5%	0.1%	1.6%	1.8%
UniStud	1.1%	0.2%	1.3%	1.0%	0.2%	1.2%	1.3%
Retirees	0.3%	0.3%	0.7%	0.2%	0.3%	0.5%	0.7%
W, Wx, H	1.1%	0.8%	1.9%	1.1%	0.7%	1.8%	1.9%
L, Lx	1.2%	0.8%	2.0%	1.1%	0.8%	1.9%	2.0%
E, S, B, Bx	0.8%	0.6%	1.4%	0.7%	0.6%	1.3%	1.4%
Se, Sv, Ss, U, Ux	1.2%	0.3%	1.5%	1.1%	0.4%	1.5%	1.6%
C, K	0.7%	0.5%	1.2%	0.7%	0.5%	1.2%	1.1%

Table A.15
Average trip travel distance and time per mode and SQV. Internal travel only.

Indicator	Mode	Observed	Diff. model	SQV	Simp. model	SQV
Travel distance [km]	total	4.58	4.43	97%	4.43	97%
	walking	1.29	1.05	91%	1.05	91%
	bicycle	4.81	4.50	94%	4.29	90%
	car driver	5.99	5.44	91%	5.44	91%
	car passenger	5.21	5.17	99%	5.17	99%
	public transport	5.88	5.28	90%	5.27	90%
Travel time [min]	total	19.62	21.79	90%	21.72	90%
	walking	18.13	16.29	91%	16.26	91%
	bicycle	20.87	17.18	84%	17.73	86%
	car driver	17.19	16.37	96%	16.34	95%
	car passenger	16.18	14.09	89%	14.06	89%
	public transport	34.02	46.26	67%	46.17	67%

Table A.16
Travel distance distributions in the mobility survey, differentiated model and simplified model. Internal travel only.

Mode	Class [km]	Observed	Diff. model	CR	Simp. model	CR
Total	(0, 0.7)	10.0%	8.3%		8.3%	
	[0.7, 1)	10.0%	5.3%		5.3%	
	[1, 1.8)	10.0%	12.8%		12.8%	
	[1.8, 2.2)	10.0%	5.6%		5.6%	
	[2.2, 3)	10.0%	10.3%		10.3%	
	[3, 4)	10.0%	11.6%		11.6%	
	[4, 5)	10.0%	9.9%		9.9%	
	[5, 7)	10.0%	15.3%		15.3%	
	[7, 10)	10.0%	13.6%		13.6%	
	[10, 657]	10.0%	7.3%	76%	7.3%	76%
Walking	(0, 0.3)	10.0%	11.8%		11.8%	
	[0.3, 0.5)	10.0%	9.8%		9.8%	
	[0.5, 0.6)	10.0%	6.3%		6.3%	
	[0.6, 0.9)	10.0%	19.1%		19.1%	
	[0.9, 1)	10.0%	6.6%		6.6%	
	[1, 1)	10.0%	0.0%		0.0%	
	[1, 1.5)	10.0%	23.5%		23.5%	
	[1.5, 2)	10.0%	12.9%		12.9%	
	[2, 2.6)	10.0%	6.6%		6.5%	
	[2.7, 12]	10.1%	3.5%	57%	3.4%	57%

(*continued on next page*)

Table A.16 (*continued*).

Mode	Class [km]	Observed	Diff. model	CR	Simp. model	CR
Bicycle	(0.07, 1)	10.0%	11.6%		10.3%	
	[1, 1.5)	9.9%	6.8%		6.1%	
	[1.5, 2)	10.0%	7.2%		6.7%	
	[2, 2.5)	10.0%	6.5%		6.2%	
	[2.5, 3.3)	10.0%	10.6%		10.3%	
	[3.3, 4)	10.1%	9.7%		9.6%	
	[4, 5)	10.0%	12.0%		12.2%	
	[5, 7.4)	9.9%	21.5%		22.7%	
	[7.5, 10)	10.1%	10.1%		11.0%	
	[10, 45)]	9.9%	4.2%	73%	4.8%	72%
Car driver	(0, 1.5)	10.0%	6.8%		6.8%	
	[1.5, 2)	10.0%	5.5%		5.5%	
	[2, 3)	10.0%	14.2%		14.2%	
	[3, 3.6)	10.0%	8.8%		8.8%	
	[3.6, 4.5)	10.0%	11.8%		11.8%	
	[4.5, 5.3)	10.0%	9.2%		9.2%	
	[5.3, 7)	10.0%	15.9%		15.9%	
	[7, 9)	10.0%	13.8%		13.8%	
	[9, 12)	10.0%	9.2%		9.2%	
	[12, 300]	10.0%	4.9%	73%	4.9%	73%
Car passenger	(0.1, 1.3)	9.9%	4.3%		4.3%	
	[1.3, 2)	10.0%	8.7%		8.7%	
	[2, 2.8)	10.1%	13.2%		13.2%	
	[2.8, 3)	10.0%	3.3%		3.3%	
	[3, 4)	10.1%	15.0%		15.0%	
	[4, 5)	9.9%	12.6%		12.6%	
	[5, 6)	10.0%	9.9%		9.9%	
	[6, 8)	9.9%	15.1%		15.1%	
	[8, 10)	10.1%	9.6%		9.6%	
	[10, 70]	10.1%	8.3%	72%	8.3%	72%
Public transport	(0.1, 1.7)	9.9%	8.0%		8.0%	
	[1.8, 2)	10.0%	3.7%		3.7%	
	[2, 3)	9.9%	15.0%		15.1%	
	[3, 3.5)	10.1%	7.1%		7.2%	
	[3.5, 4)	10.1%	7.5%		7.5%	
	[4, 5)	10.0%	12.7%		12.7%	
	[5, 6)	9.9%	11.9%		11.9%	
	[6, 7.1)	10.1%	10.1%		10.1%	
	[7.2, 10)	10.0%	15.7%		15.6%	
	[10, 657]	10.1%	8.4%	73%	8.3%	73%

Table A.17
Travel time distributions in the mobility survey, differentiated model and simplified model. Internal travel only. Classes with zero-width intervals (e.g., 20 to 20 min) due to survey methodology were merged with the next-higher class.

Mode	Class [min]	Observed	Diff. model	CR	Simp. model	CR
Total	(0.0, 5.0)	10.0%	10.2%		10.2%	
	[5.0, 10.0)	20.0%	20.0%		20.0%	
	[10.0, 15.0)	20.0%	20.0%		20.0%	
	[15.0, 20)	20.0%	20.0%		20.0%	
	[20.0, 35.0)	20.0%	23.3%		23.3%	
	[35.0, 690.0)	10.0%	15.8%	83%	15.7%	83%
Walking	(0.0, 5.0)	10.0%	6.7%		6.7%	
	[5.0, 7.0)	10.0%	10.2%		10.2%	
	[7.0, 10.0)	20.0%	15.1%		15.1%	
	[10.0, 15.0)	20.0%	21.3%		21.3%	
	[15.0, 20.0)	10.0%	17.3%		17.3%	
	[20.0, 25.0)	10.0%	12.4%		12.4%	
	[25.0, 30.0)	10.0%	7.5%		7.5%	
	[30.0, 325.0]	10.0%	9.4%	80%	9.4%	80%

(*continued on next page*)

Table A.17 (*continued*).

Mode	Class [min]	Observed	Diff. model	CR	Simp. model	CR
Bicycle	(0.0, 5.0)	10.0%	14.3%		13.9%	
	[5.0, 10.0)	20.0%	16.4%		16.8%	
	[10.0, 15.0)	19.9%	16.4%		17.4%	
	[15.0, 20.0)	10.2%	15.1%		15.5%	
	[20.0, 25.0)	10.0%	11.9%		13.1%	
	[25.0, 30.0)	9.9%	10.8%		10.8%	
	[30.0, 40.0)	10.0%	10.2%		8.5%	
	[40.0, 120.0]	10.0%	4.9%	78%	3.9%	77%
Car driver	(0.0, 5.0)	10.0%	14.0%		14.0%	
	[5.0, 10.0)	20.0%	20.9%		20.9%	
	[10.0, 13.0)	10.0%	13.1%		13.0%	
	[13.0, 15.0)	10.0%	7.8%		7.9%	
	[15.0, 20.0)	20.0%	16.1%		16.1%	
	[20.0, 30.0)	20.0%	18.2%		18.3%	
	[30.0, 615.0]	10.0%	10.0%	85%	9.9%	85%
Car passenger	(0.0, 5.0)	10.0%	17.4%		17.4%	
	[5.0, 10.0)	19.9%	23.8%		23.8%	
	[10.0, 12.0)	9.9%	8.9%		8.8%	
	[12.0, 15.0)	10.1%	12.1%		12.2%	
	[15.0, 20.0)	20.1%	15.4%		15.3%	
	[20.0, 30.0)	20.1%	15.8%		15.8%	
	[30.0, 155.0]	10.1%	6.7%	77%	6.6%	76%
Public transport	(0.0, 14.0)	9.9%	4.5%		4.5%	
	[14.0, 20.0)	10.0%	9.2%		9.2%	
	[20.0, 22.0)	10.0%	2.9%		2.9%	
	[22.0, 25.0)	10.0%	4.6%		4.6%	
	[25.0, 30.0)	10.0%	8.6%		8.6%	
	[30.0, 35.0)	10.1%	9.6%		9.7%	
	[35.0, 40.0)	10.0%	7.5%		7.5%	
	[40.0, 45.0)	10.0%	6.4%		6.4%	
	[46.0, 60.0)	9.9%	17.4%		17.4%	
	[60.0, 590.0]	10.1%	29.3%	58%	29.1%	58%

Table A.18
Observed and modeled bicycle average weekday traffic (AWT) and scalable quality value (SQV) at the 17 counting locations.

Counting location	Observed	Diff. model				Simp. model	
	bicycle	c-bike	e-bike	bicycle	SQV	bicycle	SQV
1	236	141	111	252	99%	249	99%
2	439	97	74	171	89%	175	89%
3	238	167	151	317	95%	311	95%
4	882	292	203	496	88%	543	90%
5	974	543	459	1003	99%	913	98%
6	509	294	193	487	99%	706	92%
7	868	438	415	852	99%	710	95%
8	1439	526	501	1028	90%	837	86%
9	234	82	73	154	95%	164	96%
10	295	58	81	139	92%	99	90%
11	106	15	8	23	93%	27	93%
12	159	44	17	61	93%	102	96%
13	2150	1697	1359	3055	84%	2961	85%
14	3191	2079	1602	3681	92%	3521	94%
15	1187	1157	914	2071	80%	1840	84%
16	385	157	80	238	93%	394	100%
17	722	12	5	18	79%	22	79%

Data availability

The data that has been used is confidential.

References

Argyros, D., Jensen, A.F., Rich, J., Dalyot, S., 2024. Riding smooth: A cost-benefit assessment of surface quality on copenhagen's bicycle network. Sustain. Cities Soc. 108, 105473. http://dx.doi.org/10.1016/j.scs.2024.105473.

Arning, L., Kaths, H., 2025a. Further, steeper, greener: Implications from an electric bicycle mode choice model. Int. J. Sustain. Transp. 1–16. http://dx.doi.org/10.1080/15568318.2025.2533307.

Arning, L., Kaths, H., 2025b. Just another bike? Modelling the interdependence of conventional and electric bicycle ownership and the influence of topography using large-scale travel survey data from Germany. In press. PLoS One.

Arning, L., Silva, C., Kaths, H., 2023. Review of current practice and research on E-bikes in transport models. Transp. Res. Rec. (2677(12)), 436–448. http://dx.doi.org/10.1177/03611981231168848.

Bezirksregierung Köln, 2025. Digitales geländemodell. URL https://www.bezreg-koeln.nrw.de/geobasis-nrw/produkte-und-dienste/hoehenmodelle/digitale-gelaendemodelle/digitales-gelaendemodell.

Bigazzi, A., Wong, K., 2020. Electric bicycle mode substitution for driving, public transit, conventional cycling, and walking. Transp. Res. Part D: Transp. Environ. 85, 102412. http://dx.doi.org/10.1016/j.trd.2020.102412.

Bourne, J.E., Cooper, A.R., Kelly, P., Kinnear, F.J., England, C., Leary, S., Page, A., 2020. The impact of e-cycling on travel behaviour: A scoping review. J. Transp. Heal. 19, 100910. http://dx.doi.org/10.1016/j.jth.2020.100910.

Broach, J., Dill, J., Gliebe, J., 2012. Where do cyclists ride? A route choice model developed with revealed preference GPS data. Transp. Res. Part A: Policy Pr. 46 (10), 1730–1740. http://dx.doi.org/10.1016/j.tra.2012.07.005.

Cambridge Systematics, Inc., 2010. Travel Model Validation and Reasonability Checking Manual, second ed. Federal Highway Administration, URL https://trid.trb.org/View/1600900.

Cho, S.-H., Shin, D., 2022. Estimation of route choice behaviors of bike-sharing users as first- and last-mile trips for introduction of mobility-as-a-service (MaaS). KSCE J. Civ. Eng. 26 (7), 3102–3113. http://dx.doi.org/10.1007/s12205-022-0802-1.

Chung, J., Yao, E., Pan, L., Ko, J., 2024. Understanding the route choice preferences of private and dock-based public bike users using GPS data in Seoul, South Korea. J. Transp. Geogr. 116, 103845. http://dx.doi.org/10.1016/j.jtrangeo.2024.103845.

Dane, G., Feng, T., Luub, F., Arentze, T., 2020. Route choice decisions of E-bike users: Analysis of GPS tracking data in the netherlands. In: Kyriakidis, P., Hadjimitsis, D., Skarlatos, D., Mansourian, A. (Eds.), Geospatial Technologies for Local and Regional Development. In: Lecture Notes in Geoinformation and Cartography, Springer International Publishing, Cham, pp. 109–124. http://dx.doi.org/10.1007/978-3-030-14745-7_7.

de Jong, T., Böcker, L., Weber, C., 2023. Road infrastructures, spatial surroundings, and the demand and route choices for cycling: Evidence from a GPS-based mode detection study from Oslo, Norway. Environ. Plan. B: Urban Anal. City Sci. 50 (8), 2133–2150. http://dx.doi.org/10.1177/23998083221141431.

de Melo, L.E.A., Isler, C.A., 2023. Integrating link count data for enhanced estimation of deterrence functions: A case study of short-term bicycle network interventions. J. Transp. Geogr. 112, 103711. http://dx.doi.org/10.1016/j.jtrangeo.2023.103711.

den Hoed, W., 2025. Beyond infrastructure: The multiple barriers to cycling in middle and older age. J. Transp. Heal. 41, 102003. http://dx.doi.org/10.1016/j.jth.2025.102003.

Düsseldorf, L., 2025. Radverkehr in zahlen. URL https://www.duesseldorf.de/radverkehr/fahrradzaehlstellen.

Elvik, R., Goel, R., 2019. Safety-in-numbers: An updated meta-analysis of estimates. Accid. Anal. Prev. 129, 136–147. http://dx.doi.org/10.1016/j.aap.2019.05.019.

Fan, Z., Harper, C.D., 2022. Congestion and environmental impacts of short car trip replacement with micromobility modes. Transp. Res. Part D: Transp. Environ. 103, 103173. http://dx.doi.org/10.1016/j.trd.2022.103173.

Friedrich, M., Pestel, E., Pillat, J., Heidl, U., Schiller, C., Simon, R., 2019. Anforderungen an städtische verkehrsnachfragemodelle: FE-Nr. 70.919/2015. URL https://fops.de/wp-content/uploads/2021/02/FE-70.0919-2015-Anf-an-staedt-Verkehrsnachfragemodelle-Schlussbericht.pdf.

Hallberg, M., Rasmussen, T.K., Rich, J., 2021. Modelling the impact of cycle superhighways and electric bicycles. Transp. Res. Part A: Policy Pr. 149, 397–418. http://dx.doi.org/10.1016/j.tra.2021.04.015.

Hardinghaus, M., Weschke, J., 2022. Attractive infrastructure for everyone? Different preferences for route characteristics among cyclists. Transp. Res. Part D: Transp. Environ. 111, 103465. http://dx.doi.org/10.1016/j.trd.2022.103465.

Hardinghaus, M., Weschke, J., 2023. Transforming bicycle market: Assessing cyclists route preferences on different bike types in a choice experiment. Transp. Res. Interdiscip. Perspect. 22, 100921. http://dx.doi.org/10.1016/j.trip.2023.100921.

Hebenstreit, C., 2021. Agent-Based Modelling of Bicycle Traffic and Bike Sharing (Ph.D. thesis). TU Graz.

Huber, S., Lißner, S., Lindemann, P., Muthmann, K., Schnabel, A., Friedl, J., 2021. Modelling bicycle route choice in german cities using open data, mnl and the bikesim web-app. In: 2021 7th International Conference on Models and Technologies for Intelligent Transportation Systems. MT-ITS, IEEE, pp. 1–6. http://dx.doi.org/10.1109/MT-ITS49943.2021.9529273.

Jacyna, M., Wasiak, M., Kłodawski, M., Gołębiowski, P., 2017. Modelling of bicycle traffic in the cities using VISUM. Procedia Eng. 187, 435–441. http://dx.doi.org/10.1016/j.proeng.2017.04.397.

Jafari, A., Both, A., Singh, D., Gunn, L., Giles-Corti, B., 2022. Building the road network for city-scale active transport simulation models. Simul. Model. Pr. Theory 114, 102398. http://dx.doi.org/10.1016/j.simpat.2021.102398.

Kaziyeva, D., Loidl, M., Wallentin, G., 2021. Simulating spatio-temporal patterns of bicycle flows with an agent-based model. ISPRS Int. J. Geo-Inf. 10 (2), 88. http://dx.doi.org/10.3390/ijgi10020088.

Khavarian, K., Vosough, S., Roncoli, C., 2024. Bike users' route choice behaviour: Expectations from electric bikes versus reality in Greater Helsinki. J. Cycl. Micromobility Res. 2, 100045. http://dx.doi.org/10.1016/j.jcmr.2024.100045.

Koch, T., Dugundji, E., 2021. Limitations of recursive logit for inverse reinforcement learning of bicycle route choice behavior in Amsterdam. Procedia Comput. Sci. 184, 492–499. http://dx.doi.org/10.1016/j.procs.2021.03.062.

Liu, C., Tapani, A., Kristoffersson, I., Rydergren, C., Jonsson, D., 2020. Development of a large-scale transport model with focus on cycling. Transp. Res. Part A: Policy Pr. 134, 164–183. http://dx.doi.org/10.1016/j.tra.2020.02.010.

Liu, C., Tapani, A., Kristoffersson, I., Rydergren, C., Jonsson, D., 2021. Appraisal of cycling infrastructure investments using a transport model with focus on cycling. Case Stud. Transp. Policy 9 (1), 125–136. http://dx.doi.org/10.1016/j.cstp.2020.11.003.

Loidl, M., Zagel, B., 2014. Assessing bicycle safety in multiple networks with different data models. In: Vogler, R., Adrijana, C., Strobl, J., Gerald, G. (Eds.), GI_Forum 2014 – Geospatial Innovation for Society. Austrian Academy of Sciences Press, Vienna, pp. 144–154. http://dx.doi.org/10.1553/giscience2014s144.

Łukawska, M., 2024. Quantitative modelling of cyclists' route choice behaviour on utilitarian trips based on GPS data: associated factors and behavioural implications. Transp. Rev. 44 (5), 1045–1076. http://dx.doi.org/10.1080/01441647.2024.2355468.

Łukawska, M., Paulsen, M., Rasmussen, T.K., Jensen, A.F., Nielsen, O.A., 2023. A joint bicycle route choice model for various cycling frequencies and trip distances based on a large crowdsourced GPS dataset. Transp. Res. Part A, Policy Pr. 176, 103834. http://dx.doi.org/10.1016/j.tra.2023.103834.

Meister, A., Felder, M., Schmid, B., Axhausen, K.W., 2023. Route choice modeling for cyclists on urban networks. Transp. Res. Part A: Policy Pr. 173, 103723. http://dx.doi.org/10.1016/j.tra.2023.103723.

Meister, A., Liang, Z., Felder, M., Axhausen, K.W., 2024. Comparative study of route choice models for cyclists. J. Cycl. Micromobility Res. 2, 100018. http://dx.doi.org/10.1016/j.jcmr.2024.100018.

Oskarbski, J., Birr, K., Żarski, K., 2021. Bicycle traffic model for sustainable urban mobility planning. Energies 14 (18), 5970. http://dx.doi.org/10.3390/en14185970.

Paulsen, M., Rich, J., 2023. Societally optimal expansion of bicycle networks. Transp. Res. Part B: Methodol. 174, 102778. http://dx.doi.org/10.1016/j.trb.2023.06.002.

Paulsen, M., Rich, J., 2024. Welfare optimal bicycle network expansions with induced demand. Transp. Res. Part B: Methodol. 190, 103095. http://dx.doi.org/10.1016/j.trb.2024.103095.

Pestel, E., 2021. Qualität von Verkehrsnachfragemodellen (Ph.D. thesis). University of Stuttgart, http://dx.doi.org/10.18419/opus-11752.

Prato, C.G., Halldórsdóttir, K., Nielsen, O.A., 2018. Evaluation of land-use and transport network effects on cyclists' route choices in the copenhagen region in value-of-distance space. Int. J. Sustain. Transp. 12 (10), 770–781. http://dx.doi.org/10.1080/15568318.2018.1437236.

Reckermann, H., Gutjar, M., Kowald, M., 2024. Studying shared bike route choice behavior using a bike-sharing system in Germany. J. Cycl. Micromobility Res. 2, 100017. http://dx.doi.org/10.1016/j.jcmr.2024.100017.

Rich, J., Jensen, A.F., Pilegaard, N., Hallberg, M., 2021. Cost-benefit of bicycle infrastructure with e-bikes and cycle superhighways. Case Stud. Transp. Policy 9 (2), 608–615. http://dx.doi.org/10.1016/j.cstp.2021.02.015.

Rupi, F., Freo, M., Poliziani, C., Postorino, M.N., Schweizer, J., 2023. Analysis of gender-specific bicycle route choices using revealed preference surveys based on GPS traces. Transp. Policy 133, 1–14. http://dx.doi.org/10.1016/j.tranpol.2023.01.001.

Scott, D.M., Lu, W., Brown, M.J., 2021. Route choice of bike share users: Leveraging GPS data to derive choice sets. J. Transp. Geogr. 90, 102903. http://dx.doi.org/10.1016/j.jtrangeo.2020.102903.

Senatsverwaltung für Mobilität, Verkehr, Klimaschutz und Umwelt, 2024. Zählstellen und fahrradbarometer: Fahrradverkehr in zahlen. URL https://www.berlin.de/sen/uvk/mobilitaet-und-verkehr/verkehrsplanung/radverkehr/weitere-radinfrastruktur/zaehlstellen-und-fahrradbarometer/.

Shah, N.R., Cherry, C.R., 2021. Different safety awareness and route choice between frequent and infrequent bicyclists: Findings from revealed preference study using bikeshare data. Transp. Res. Rec.: J. Transp. Res. Board 2675 (11), 269–279. http://dx.doi.org/10.1177/03611981211017136.

Stadt Wuppertal, 2021. Wuppertaler mobilitätsbefragung 2020. URL https://www.wuppertal.de/rathaus-buergerservice/verkehr/mobil_sein/mobilitaetsbefragung.php.

van Dulmen, A., Fellendorf, M., 2021. Regional bicycle network evaluation and strategic planning: A quantitative methodological approach despite limited data sources for cycling. Transp. Res. Rec.: J. Transp. Res. Board 2675 (12), 306–316. http://dx.doi.org/10.1177/03611981211028870.

Ziemke, D., Metzler, S., Nagel, K., 2019. Bicycle traffic and its interaction with motorized traffic in an agent-based transport simulation framework. Future Gener. Comput. Syst. 97, 30–40. http://dx.doi.org/10.1016/j.future.2018.11.005.